



HAL
open science

Uncyclized xanthommatin is a key ommochrome intermediate in invertebrate coloration

Florent Figon, Thibaut Munsch, Cecile Croix, Marie-Claude Viaud-Massuard, Arnaud Lanoue, Jérôme Casas

► **To cite this version:**

Florent Figon, Thibaut Munsch, Cecile Croix, Marie-Claude Viaud-Massuard, Arnaud Lanoue, et al.. Uncyclized xanthommatin is a key ommochrome intermediate in invertebrate coloration. *Insect Biochemistry and Molecular Biology*, 2020, 124, pp.103403. 10.1016/j.ibmb.2020.103403 . hal-02886293

HAL Id: hal-02886293

<https://univ-tours.hal.science/hal-02886293>

Submitted on 22 Aug 2022

HAL is a multi-disciplinary open access archive for the deposit and dissemination of scientific research documents, whether they are published or not. The documents may come from teaching and research institutions in France or abroad, or from public or private research centers.

L'archive ouverte pluridisciplinaire **HAL**, est destinée au dépôt et à la diffusion de documents scientifiques de niveau recherche, publiés ou non, émanant des établissements d'enseignement et de recherche français ou étrangers, des laboratoires publics ou privés.



Distributed under a Creative Commons Attribution - NonCommercial 4.0 International License

1 Uncyclized xanthommatin is a key ommochrome intermediate in invertebrate coloration

2 **Short title:** Uncyclized xanthommatin in ommochrome biosynthesis

3 **Florent Figon^{1*}, Thibaut Munsch², Cécile Croix³, Marie-Claude Viaud-Massuard³, Arnaud**
4 **Lanoue², and Jérôme Casas¹**

5 From the ¹Institut de Recherche sur la Biologie de l’Insecte, UMR CNRS 7261, Université de Tours,
6 37200 Tours, France; ²Biomolécules et Biotechnologies Végétales, EA 2106, Université de Tours,
7 37200 Tours, France; ³Génétique, Immunothérapie, Chimie et Cancer, UMR CNRS 7292, Université
8 de Tours, 37200 Tours, France

9 *To whom correspondence should be addressed: Florent Figon: Institut de Recherche sur la Biologie
10 de l’Insecte, UMR CNRS 7261, Université de Tours, 37200 Tours, France; florent.figon@univ-
11 tours.fr; Tel. +33 (0)2 47 36 69 81; Fax. +33 (0)2 47 36 69 66.

12 **Author contributions:** F. F., A. L. and J. C. conceptualization; F. F. data curation; F. F. formal
13 analysis; M.-C. V.-M., A. L. and J. C. funding acquisition; F. F., T. M. and C. C. investigation; F. F.,
14 T. M., C. C., A. L. and J. C. methodology; F. F., A. L. and J. C. project administration; M.-C. V.-M.,
15 A. L. and J. C. resources; J. C. supervision; F. F., A. L. and J. C. validation; F. F. visualization; F. F.
16 and J. C. writing – original draft; F. F., T. M., C. C., M.-C. V.-M., A. L. and J. C. writing – review &
17 editing.

18 **Abbreviations:** CE, collision energy; CV, cone voltage; DAD, diode-array detector; ESI⁺, positive-
19 mode electron spray ionization; LC, liquid chromatography; MeOH-HCl, acidified methanol with 0.5
20 % hydrochloric acid; MRM, multiple reaction monitoring; MS, mass spectrometry; MS/MS, tandem
21 mass spectrometry; MW, molecular weight; *m/z*, mass-to-charge ratio; NMR, nuclear magnetic
22 resonance; RT, retention time; SD, standard deviation; SE, standard error; SIR, single ion recording;
23 UV, ultraviolet.

24 **Abstract**

25 Ommochromes are widespread pigments that mediate multiple functions in invertebrates. The two
26 main families of ommochromes are ommatins and ommins, which both originate from the kynurenine
27 pathway but differ in their backbone, thereby in their coloration and function. Despite its broad
28 significance, how the structural diversity of ommochromes arises *in vivo* has remained an open
29 question since their first description. In this study, we combined organic synthesis, analytical
30 chemistry and organelle purification to address this issue. From a set of synthesized ommatins, we
31 derived a fragmentation pattern that helped elucidating the structure of new ommochromes. We
32 identified uncyclized xanthommatin as the elusive biological intermediate that links the kynurenine
33 pathway to the ommatin pathway within ommochromosomes, the ommochrome-producing organelles.
34 Due to its unique structure, we propose that uncyclized xanthommatin functions as a key branching
35 metabolite in the biosynthesis and structural diversification of ommatins and ommins, from insects to
36 cephalopods.

37 **Keywords:** high-performance liquid chromatography (HPLC), kynurenine, mass spectrometry (MS),
38 ommin, ommochromosome, ultraviolet-visible spectroscopy (UV-Vis spectroscopy)

39 **1. Introduction**

40 Ommochromes are widespread phenoxazinone pigments of invertebrates. They act as light filters in
41 compound eyes and determine the integumental coloration of a large range of invertebrates (Figon and
42 Casas, 2019). Ommochromes are also of particular interest in applied sciences as their scaffold has
43 been used to design antitumor agents (Bolognese et al., 2002) and, very recently, to manufacture
44 biomimetic color changing electrochromic devices (Kumar et al., 2018). The two major families of
45 natural ommochromes are the yellow-to-red ommatins and the purple ommins that contain a
46 supplemental phenothiazine ring. Ommatins are currently the best described family of ommochromes
47 and occur throughout invertebrates. Ommins are much less characterized, although they are virtually
48 ubiquitous in insects and cephalopods (Needham, 1974; Riddiford and Ajami, 1971). After nearly 80

49 years and despite their broad significance, the structural and chemical relationships between these two
50 abundant families of ommochromes remain surprisingly mysterious (Figon and Casas, 2019).

51 The early steps of the biosynthesis of ommochromes in invertebrates cover the oxidation of
52 tryptophan into kynurenines (Fig 1B) (Figon and Casas, 2019), from insects (Linzen, 1974) and
53 spiders (Croucher et al., 2013) to planarians (Stubenhaus et al., 2016) and cephalopods (Williams et
54 al., 2019b). These oxidative steps are homologous to the kynurenine pathway of vertebrates in which
55 the last enzyme, the mitochondria-bound kynurenine 3-monooxygenase, catalyzes the formation of 3-
56 hydroxykynurenine. This *ortho*-aminophenolic amino acid is the currently accepted last common
57 precursor of all known ommochromes, from ommatins to ommins (Fig 1B) (Figon and Casas, 2019).
58 The catabolism of tryptophan then diverges from vertebrates because invertebrates lack the glutarate
59 pathway but possess the ommochrome pathway (Linzen, 1974).

60 Ommochromes are produced within specialized intracellular organelles, called
61 ommochromosomes, most likely after the incorporation of 3-hydroxykynurenine (Figon and Casas,
62 2019; Mackenzie et al., 2000). Two hypotheses have been proposed to explain how ommatins
63 originate from there. (1) It has been suggested very early, but on weak evidence, that the oxidative
64 dimerization of 3-hydroxykynurenine into uncyclized xanthommatin and its subsequent intramolecular
65 cyclization account for the biosynthesis of ommochromes (Fig 1B) (Butenandt and Schäfer, 1962). (2)
66 The condensation of *ortho*-aminophenols with xanthurenic acid has been proposed to form directly the
67 oxo-pyrido[3,2-*a*]phenoxazinone chromophore of ommatins (Fig 1B) (Linzen, 1974; Panettieri et al.,
68 2018). Hypothesis 1 is currently more accepted because ommatins can be synthesized *in vitro* by the
69 oxidative condensation of 3-hydroxykynurenine, which is predicted to form an unstable intermediate,
70 the 3-hydroxykynurenine dimer called uncyclized xanthommatin (Butenandt and Schäfer, 1962; Figon
71 and Casas, 2019; Iwahashi and Ishii, 1997; Williams et al., 2019a; Zhuravlev et al., 2018).
72 Furthermore, uncyclized xanthommatin was speculated in biological extracts (Bolognese and
73 Scherillo, 1974), putatively identified in the *in vitro* oxidation of 3-hydroxykynurenine (Iwahashi and
74 Ishii, 1997) and its enzymatic formation predicted *in silico* by quantum calculations (Zhuravlev et al.,

75 2018). However, it has never been formerly extracted and characterized in biological samples.
76 Alternatively, hypothesis 2 does not involve the formation of any intermediate between the kynurenine
77 pathway and the ommatin pathway. Hence, to discriminate between the two hypotheses, one needs to
78 determine whether uncyclized xanthommatin is produced *in vivo* (Fig 1B). Finding this still-elusive
79 intermediate in biological extracts would therefore be a major step in characterizing the actual
80 biosynthetic pathway of ommochromes.

81 Deciphering the ommochrome pathway requires the characterization of metabolites in
82 biological extracts. However, biological ommochromes are remarkably refractory to NMR
83 spectroscopy, partly because of their poor solubility in most conventional solvents (Bolognese et al.,
84 1988b; Crescenzi et al., 2004; Parrilli and Bolognese, 1992). It was only very recently that the first ¹H-
85 NMR spectrum of xanthommatin, whose structure has been known for 60 years, was published after
86 extensive purification and optimization steps (Kumar et al., 2018). However, from a theoretical point
87 of view, mere ¹H-NMR data cannot provide enough information on the exact structure of
88 ommochromes. Indeed, they are rather poor in carbon-bonded hydrogens, which prevents access to all
89 positions in the structure. Furthermore, they are redox/pH sensitives and prone to tautomerization,
90 which complicate ¹H spectra greatly. Since our main target compound, uncyclized xanthommatin, is
91 unstable in solution (Bolognese et al., 1988a; Bolognese and Scherillo, 1974), it is highly improbable
92 that gold-standard techniques for structural elucidation, such as ¹³C- and 2D-NMR, can be used
93 because they suffer from too low sensitivity. In order to elucidate the biological diversity of
94 ommochromes, one should therefore look for a combination of more sensitive analytical techniques
95 that provide orthogonal information, such as mass spectrometry and UV-Visible spectroscopy. For
96 nearly a decade, mass spectrometry (MS) has been used to elucidate the structure of both known and
97 unknown ommochromes from biological samples (Futahashi et al., 2012; Panettieri et al., 2018; Reiter
98 et al., 2018; Williams et al., 2016). Yet, evidence for common and compound-specific fragmentation
99 patterns of ommochromes are scarce [but see (Panettieri et al., 2018; Reiter et al., 2018)]. Together
100 with the seldom use of synthesized ommochromes, this lack of analytical data accounts for the very

101 little progress made since four decades to unravel the biological diversity of ommochromes (Figon and
102 Casas, 2019).

103 In this study, we synthesized xanthommatin and its decarboxylated form by the oxidative
104 dimerization of 3-hydroxykynurenine. Knowing that ommatins are methoxylated in acidified methanol
105 (MeOH-HCl), we incubated synthesized xanthommatin in MeOH-HCl to produce a range of ommatin-
106 derivatives. We constructed an analytical dataset of those ommatins by a combination of UV-Visible
107 spectroscopy, and (tandem) mass spectrometry after separation by liquid chromatography. From this
108 dataset, we derived a fragmentation pattern with valuable structural information, especially when
109 combined with UV-Visible spectra, to infer the structure of new ommochromes with strong
110 confidence. Hence, we could elucidate the structure of three methoxylated ommatins and, more
111 importantly, of uncyclized xanthommatin. Our experiments demonstrated that ommatins are easily and
112 rapidly methoxylated leading to artifacts in conditions matching standard extraction procedures from
113 biological samples. By combining our analytical tools with an artifact-free extraction protocol and a
114 subcellular fractionation of ommochromosomes, we reinvestigated the ommochromes of housefly
115 eyes. We could identify xanthommatin, decarboxylated xanthommatin and uncyclized xanthommatin
116 in ommochromosomes. Our results provide strong support to the hypothesis that ommatin biosynthesis
117 occurs in subcellular organelles through the dimerization of 3-hydroxykynurenine and its subsequent
118 intramolecular cyclization (hypothesis 1, Fig 1B). Furthermore, the unique structure of uncyclized
119 xanthommatin makes it a good candidate to link the biosynthetic pathways of ommatins and ommins,
120 which has important implications on how ommochromes have diversified in a wide range of
121 phylogenetically-distant species.

122 2. Material and Method

123 2.1 *Insects*

124 Houseflies (*Musca domestica*) were obtained at the pupal stage from Kreca. After hatching, houseflies
125 were either directly processed for ommochromosome purification or stored at -20 °C for ommochrome
126 extraction.

127 **2.2 Reagents**

128 Sodium dihydrogen phosphate, sodium hydrogen phosphate, L-kynurenine ($\geq 98\%$), 3-hydroxy-D,L-
129 kynurenine, trifluoroacetic acid (TFA), Triton X-100, tris(hydroxymethyl)aminomethane (Tris),
130 potassium ferricyanide, magnesium chloride, potassium chloride, potassium pentoxide and
131 cinnabaric acid ($\geq 98\%$) were purchased from Sigma-Aldrich. Methanol, potassium chloride and
132 hydrochloric acid (37%) were purchased from Carlo Erba reagents. Nycodenz® was purchased from
133 Axis Shield. L-tryptophan ($\geq 99\%$) and xanthurenic acid ($\geq 96\%$) were purchased from Acros
134 Organics. Sucrose (99%) and sulfurous acid ($\geq 6\% \text{SO}_2$) were purchased from Alfa Aesar. β -
135 Mercaptoethanol was purchased from BDH Chemicals. Acetonitrile and formic acid were purchased
136 from ThermoFischer Scientific.

137 **2.3 In vitro synthesis of xanthommatin**

138 *2.3.1 Oxidative condensation of 3-hydroxykynurenine under anoxia*

139 A mixture of ommatins was synthesized by oxidizing 3-hydroxy-D,L-kynurenine with potassium
140 ferricyanide as previously described (Butenandt et al., 1954; Hori and Riddiford, 1981), with some
141 modifications. In a round bottom flask under argon, a solution of 44.6 mM of 3-hydroxy-D,L-
142 kynurenine was prepared by dissolving 455 μmol (102 mg) in 10.2 mL of 0.2 M phosphate buffer at
143 pH 7.1 (PB). In a second round bottom flask under argon, 174 mM of potassium ferricyanide (303 mg)
144 were dissolved in 5.3 mL of PB. Both solutions were purged with argon and protected from light. The
145 potassium ferricyanide solution was added slowly to the solution of 3-hydroxy-D,L-kynurenine. The
146 resulted reaction mixture was stirred at room temperature for 1 h 30 in darkness. Then, 10 mL of
147 sulfurous acid diluted four times in PB was added. The final solution was brought to 4 °C for 30 min
148 during which red flocculants formed. The suspension was then transferred into a 50 mL centrifuge
149 tube. The round bottom flask was rinsed with 8 mL of sulfurous acid previously diluted four times in
150 PB to ensure the complete reduction and flocculation of synthesized ommatins, as well as to remove
151 ferrocyanide. The final suspension was centrifuged for 10 min at 10 000 $\times g$ and at 4 °C. The solid

152 was desiccated overnight under vacuum over potassium hydroxide and phosphorus pentoxide. 104 mg
153 of a reddish brown powder was obtained and kept at 4 °C in darkness until further use.

154 *2.3.2 Solubilization and analyses of synthesized ommatins*

155 A solution of synthesized ommatins at 1 mg/mL of was made in methanol acidified with 0.5 % HCl
156 and pre-cooled at -20 °C (MeOH-HCl). The solution was mixed for 30 s and filtered on 0.45 µm
157 filters. All steps were performed, as much as possible, at 4 °C in darkness. The overall procedure took
158 less than two minutes. Immediately after filtration, the solution was subjected to absorption and mass
159 spectrometry analysis (see below). The filtered solution was then stored at 20 °C in darkness and
160 subjected to the same analysis 24 hours later.

161 *2.4 Nuclear Magnetic Resonance (NMR) Spectroscopy*

162 One milligram of synthesized product was solubilized in 600 µL of d6-DMSO acidified with 25 µL of
163 TFA, as previously described (Kumar et al., 2018; Williams et al., 2019a). NMR spectra were
164 recorded on Bruker AVANCE AV 300 instruments and the NMR experiment was reported in units,
165 parts per million (ppm), using residual solvent peaks d6-DMSO ($\delta = 2.50$ ppm) for ¹H NMR as
166 internal reference. Multiplicities are recorded as: s = singlet, d = doublet, t = triplet, dd = doublet of
167 doublets, m = multiplet, bs = broad singlet. Coupling constants (J) are reported in hertz (Hz).

168 ¹H NMR (300 MHz, d6-DMSO + 0.04 % TFA) δ 8.37 (bs, 3H, H₁), 8.21 (bs, 1H, NH₈), 8.04 (t, J =
169 4.5 Hz, 1H, H₅), 7.83 - 7.82 (m, 2H, H₄, H₆), 7.69 (s, 1H, H₇), 6.67 (s, 1H, H₉), 4.46 - 4.42 (m, 1H,
170 H₂), 3.89 (bs, 2H, H₃).

171 *2.5 Ultra-Pressure Liquid Chromatography coupled to Diode-Array Detector and Electrospray* 172 *Ionization Source-based Mass Spectrometer (UPLC-DAD-ESI-MS)*

173 *2.5.1 System*

174 A reversed-phase ACQUITY UPLC® system coupled to a diode-array detector (DAD) and to a Xevo
175 TQD triple quadrupole mass spectrometer (MS) equipped with an electrospray ionization source (ESI)
176 was used (Waters, Milford, MA). Tandem mass spectrometry (MS/MS) was performed by collision-

177 induced dissociation with argon. Data were collected and processed using MassLynx software, version
178 4.1 (Waters, Milford, MA).

179 *2.5.2 Chromatographic conditions*

180 Analytes were separated on a CSH™ C18 column (2.1 x 150 mm, 1.7 μm) equipped with a CSH™
181 C18 VanGuard™ pre-column (2.1 x 5 mm). The column temperature was set at 45 °C and the flow
182 rate at 0.4 mL/min. The injection volume was 5 μL. The mobile phase consisted in a mixture of MilliQ
183 water (eluent A) and acetonitrile (eluent B), both prepared with 0.1 % formic acid. The linear gradient
184 was set from 2 % to 40 % B for 18 min.

185 *2.5.3 Spectroscopic conditions*

186 The MS continuously alternated between positive and negative modes every 20 ms. Capillary voltage,
187 sample cone voltage (CV) and collision energy (CE) were set at 2 000 V, 30 V and 3 eV, respectively,
188 for MS conditions. CE was set at 30 eV for tandem MS conditions. Cone and desolvation gas flow
189 rates were set at 30 and 1 000 L/h, respectively. Absorption spectra of analytes were continuously
190 recorded between 200 and 500 nm with a one-nm step. Analytes were annotated and identified
191 according to their retention times, absorbance spectra, mass spectra and tandem mass spectra (Table
192 1).

193 *2.6 Thermal reactivity of ommatins in acidified methanol in darkness*

194 *2.6.1 Conditions of solubilization and incubation*

195 Solutions (n = 5) of synthesized ommatins at 1 mg/mL were prepared in MeOH-HCl. The solutions
196 were mixed for 30 s and filtered on 0.45 μm filters. Aliquots of 50 μL were prepared for each sample
197 and stored at either 20 °C or -20 °C in darkness. All steps were performed, as much as possible, in
198 darkness and at 4 °C. The overall procedure for each sample took less than two minutes. During the
199 course of the experiment, each aliquot was analyzed only once by UPLC-ESI-MS/MS, representing a
200 single time point for each sample.

201 2.6.2 Quantification of ommatins

202 Unaltered (*i.e.* xanthommatin and its decarboxylated form) and their methoxylated forms were
203 detected and quantified by absorption and MS/MS (single reaction monitoring [MRM] mode)
204 spectrometry. MRM conditions were optimized for each ommatin based on the following parent-to-
205 product ion transitions: xanthommatin $[M+H]^+$ 424>361 m/z (CV 38 V, CE 25 eV), α^3 -methoxy-
206 xanthommatin $[M+H]^+$ 438>375 m/z (CV 37 V, CE 23 eV), α^3, α^{11} -dimethoxy-xanthommatin $[M+H]^+$
207 452>375 m/z (CV 38 V, CE 25 eV), decarboxylated xanthommatin $[M+H]^+$ 380>317 m/z (CV 34 V,
208 CE 28 eV) and decarboxylated α^{11} -methoxy-xanthommatin $[M+H]^+$ 394>317 m/z (CV 34 V, CE 28
209 eV). See Fig S2 for detailed information on MS/MS optimization. Peak areas for both absorption and
210 MRM signals were calculated by integrating chromatographic peaks with a “Mean” smoothing method
211 (window size: ± 3 scans, number of smooths: 2). Absorbance values at 414 nm of unaltered ommatins
212 were summed and reported as a percentage of the total absorbance of unaltered and methoxylated
213 ommatins. The decay at -20 °C of uncyclized xanthommatin was followed by integrating both the
214 absorbance at 430 nm and the 443 m/z SIR signals associated to the chromatographic peak of
215 uncyclized xanthommatin at RT 6.7 min.

216 2.7 Extraction and content analysis of housefly eyes

217 2.7.1 Biological extractions

218 Five housefly (*M. domestica*) heads were pooled per sample (n = 5), weighted and homogenized in 1
219 mL MeOH-HCl with a tissue grinder (four metal balls, 300 strokes/min for 1 min). The obtained crude
220 extracts were centrifuged for 5 min at 10 000 $\times g$ and 4 °C. The supernatants were filtered on 0.45 μm
221 filters and immediately processed for absorption and MS analyses. All steps were performed, as much
222 as possible, in darkness at 4 °C. The overall extraction procedure took less than 20 min.

223 2.7.2 Chromatographic profile

224 The chromatographic profile of housefly eyes that includes L-tryptophan, xanthurenic acid, 3-D,L-
225 hydroxykynurenine, uncyclized xanthommatin, xanthommatin and decarboxylated xanthommatin is
226 reported based on their optimized MRM signals. L-Tryptophan and xanthurenic acid were quantified

227 based on their optimized MRM signals: $[M+H]^+$ 205>118 m/z (CV 26 V and CE 25 eV) and $[M+H]^+$
228 206>132 m/z (CV 36 V and CE 28 eV), respectively. See Fig S2 for detailed information on MS/MS
229 optimization. 3-D,L-Hydroxykynurenine and uncyclized xanthommatin were quantified based on their
230 absorption at 370 and 430 nm, respectively. L-Tryptophan, 3-D,L-hydroxykynurenine and xanthurenic
231 acid levels were converted to molar concentrations using calibrated curves of commercial standards.
232 Molar concentrations of uncyclized xanthommatin are reported as cinnabarinic equivalent, since both
233 metabolites possess the same chromophore and presented similar absorbance spectra (see Fig 5C).

234 **2.8 Purification and content analysis of ommochromasomes**

235 *2.8.1 Isolation protocol*

236 Ommochromasomes from housefly eyes were purified as previously described (Cölln et al., 1981),
237 with slight modifications. The isolation buffer was prepared with MgCl₂ instead of CaCl₂,
238 metrizamide was replaced by Nycodenz® (iohexol) and the final ultracentrifugation step was
239 performed on Nycodenz layers solely since Nycodenz mixes with sucrose layers. See Supplemental
240 File S1 for a more detailed protocol.

241 *2.8.2 Extraction of ommochrome-related metabolites from purified ommochromasomes*

242 Pellets (n = 5) were resuspended in 50 μ L MeOH-HCl and directly subjected to UPLC-DAD-ESI-
243 MS/MS analysis. All steps were performed, as much as possible, in darkness and at 4 °C. The overall
244 extraction procedure took less than 2 min per sample.

245 *2.8.3 Metabolic analysis of purified ommochromasomes*

246 The chromatographic profile of purified ommochromasomes that includes L-tryptophan, xanthurenic
247 acid, 3-D,L-hydroxykynurenine, uncyclized xanthommatin, xanthommatin, decarboxylated
248 xanthommatin and β -mercaptoethanol-added ommatins is reported based on their optimized MRM
249 signals. L-Tryptophan, 3-D,L-hydroxykynurenine, xanthurenic acid and uncyclized xanthommatin
250 were quantified as described for crude extracts of housefly eyes.

251 **2.9 Statistical analysis**

252 Statistical analyses were performed using the R software, version 3.4.1 (www.r-project.org). Statistical
253 threshold was set to 0.05. For kinetic analyses, changes of metabolite quantities overtime were first
254 tested by correlation tests assuming monotonic variations (Sperman's rank correlation test).
255 Depending on the shape of the variation, either linear or logarithmic in this study, we performed linear
256 regressions on either unchanged or log-scaled time points, respectively. For comparisons of two
257 samples, we first assessed whether normality and homoscedasticity criteria were met with Shapiro-
258 Wilkinson normality tests and Fligner-Killeen tests of homogeneity of variances, respectively. When
259 data were heteroscedastic, we used Welch *t*-test rather than Student *t*-test. For multiple comparisons,
260 we also tested normality and heteroscedasticity. Since the normality criteria was not met in that case,
261 we performed a Kruskal-Wallis rank sum test followed by pairwise comparisons using a Wilcoxon
262 rank sum test with the Holm adjustment method. Detailed results of all statistical analyses are reported
263 in File S2.

264 **3. Results**

265 **3.1 UPLC-DAD-MS/MS structural elucidation of synthesized xanthommatin and its *in vitro***
266 ***derivatives***

267 Since xanthommatin is commercially unavailable, we achieved its *in vitro* synthesis by oxidative
268 condensation of 3-hydroxykynurenine under anoxia as previously reported (Butenandt et al., 1954).
269 ¹H-NMR spectroscopy on the product validated that the main synthesized compound was
270 xanthommatin (see Material and Methods and Fig S1) (Williams et al., 2019a). The synthesized
271 product was then solubilized in methanol acidified with 0.5 % HCl (MeOH-HCl) and analyzed by
272 Liquid Chromatography (LC) coupled to Diode-Array Detection (DAD) and Mass Spectrometry (MS)
273 (Fig 2). The product was solubilized extemporaneously to avoid any chemical degradation before LC-
274 DAD-MS analyses (Fig 2A, B). Chromatograms showed two main peaks corresponding to
275 xanthommatin (retention time [RT]: 11.8 min, [M+H]⁺ at *m/z* 424) and decarboxylated xanthommatin
276 (RT: 9.1 min, [M+H]⁺ at *m/z* 380) (Table 1). Two co-eluting peaks were present in trace amounts at

277 RT 8.5 and 11.9 min and were associated to $[M+H]^+$ at m/z 460 and $[M+H]^+$ at m/z 504, respectively.
278 The detailed analysis of this sample enabled the detection of a small peak at RT 6.7 min ($[M+H]^+$ at
279 m/z 443) with its corresponding chromatogram at 430 nm (Fig 2A). A detailed analysis of this
280 particular compound is presented further in the text.

281 Table 1. Analytical characteristics of ommatin-related compounds found *in vitro* and in biological extracts.

Annotation (Formula, calculated MW)	RT (min)	Absorbance peaks	Monocharged ions (<i>m/z</i> loss)	Double-charged ions (<i>m/z</i> loss)	MS/MS fragments (<i>m/z</i> loss)
<i>Detected in synthesized ommatins, crude extracts of housefly eyes and ommochromasome extracts</i>					
3-Hydroxykynurenine (C ₁₀ H ₁₂ N ₂ O ₄ , 224.21)	1.6	231; 264; 376	224.9 [M+H] ⁺ ; 207.9 (-17); 161.9 (-63); 152.0 (-73)	Not detected	207.7 (-17); 161.9 (- 63)
Uncyclized xanthommatin (C ₂₀ H ₁₈ N ₄ O ₈ , 442.38)	6.7	235; 420- 450	442.9 [M+H] ⁺ ; 425.9 (-17); 408.8 (-34); 353.0 (-90)	213.6 [M- 17+2H] ²⁺	425.9 (-17); 409.0 (- 34); 390.9 (-52); 363.1 (-80); 353.0 (-90); 344.9 (-98); 335.1 (- 108); 317.0 (-126); 307.0 (-136)
Xanthommatin (C ₂₀ H ₁₃ N ₃ O ₈ , 423.33)	11.8	234; 442	423.9 [M+H] ⁺ ; 406.8 (-17); 377.9 (-46); 350.9 (-73)	212.5 [M+2H] ²⁺ ; 189.5 (-23)	406.3 (-17; -18); 360.7 (-63); 350.8 (-73); 316.8 (-107); 304.8 (- 119); 288.9 (-135)
Decarboxylated xanthommatin (C ₁₉ H ₁₃ N ₃ O ₆ , 379.32)	9.1	234; 442	379.9 [M+H] ⁺ ; 362.9 (-17); 333.9 (-46); 306.9 (-73)	190.5 [M+2H] ²⁺ ; 167.5 (-23)	362.7 (-17; -18); 333.7 (-46); 316.8 (-63); 306.8 (-73); 290.9 (- 89)
<i>Only detected in synthesized ommatins</i>					
Xanthommatin sulphate/phosphate ester (C ₂₀ H ₁₃ N ₃ O ₁₁ S, 503.40; C ₂₀ H ₁₄ N ₃ O ₁₁ P, 503.31)	12.4	236; 445	503.9 [M+H] ⁺ ; 453.6 (-50); 430.5 (-73?); 379.8 (- 124); 350.7 (-153)	252.5 [M+2H] ²⁺ ; 229.5 (-23)	487.0 (-17); 440.6 (- 63); 430.8 (-73); 422.8 (-81); 396.5 (-107?); 384.9 (-119)
Decarboxylated xanthommatin sulphate/phosphate ester (C ₁₉ H ₁₃ N ₃ O ₉ S, 459.39; C ₁₉ H ₁₄ N ₃ O ₉ P, 459.30)	8.5	236; 443	459.8 [M+H] ⁺ ; 442.8 (-17); 413.8 (-46); 386.7 (-73)	230.4 [M+2H] ²⁺ ; 207.4 (-23)	442.8 (-17); 413.7 (- 46); 396.8 (-63); 386.8 (-73)
<i>Detected in synthesized ommatins incubated in MeOH-HCl in darkness</i>					
α ³ -Methoxy-xanthommatin (C ₂₁ H ₁₅ N ₃ O ₈ , 437.36)	12.6	217; 303; 452	437.9 [M+H] ⁺ ; 420.9 (-17); 391.9 (-46); 364.9 (-73)	219.4 [M+2H] ²⁺ ; 196.5 (-23)	420.7 (-17); 391.8 (- 46); 374.8 (-63); 364.8 (-73); 314.8 (-123); 304.8 (-133)
α ³ , α ¹¹ -Dimethoxy- xanthommatin (C ₂₂ H ₁₇ N ₃ O ₈ , 451.39)	13.0	217; 303; 452	451.9 [M+H] ⁺ ; 434.9 (-17); 391.9 (-60); 364.9 (-87)	226.5 [M+2H] ²⁺ ; 196.4 (-30)	434.9 (-17); 374.8 (- 77); 364.9 (-87); 314.8 (-137); 304.8 (-147)
Decarboxylated α ¹¹ - methoxy-xanthommatin (C ₂₀ H ₁₅ N ₃ O ₆ , 393.35)	10.1	234; 442	393.9 [M+H] ⁺ ; 376.9 (-17); 333.9 (-60); 307.0 (-87)	197.6 [M+2H] ²⁺ ; 167.4 (-30)	376.7 (-17; -18); 333.8 (-60); 316.8 (-77); 306.9 (-87); 290.9 (- 105)
Unknown altered xanthommatin (455)	14.4	242; 442	455.9 [M+H] ⁺	228.4 [M+2H] ²⁺ ; 205.4 (-23)	340.1 (-116); 324.6 (- 131?); 295.0 (-161); 205.2 (-251)
Unknown altered methoxy- xanthommatin (469)	14.9	243; 390; 452	469.8 [M+H] ⁺	235.5 [M+2H] ²⁺ ; 212.4 (-23)	353.7 (-116); 338.8 (- 131); 294.7 (-175); 204.8 (-265)
Unknown altered dimethoxy-xanthommatin (483)	15.0	242; 388; 450	484.0 [M+H] ⁺	242.5 [M+2H] ²⁺ ; 212.5 (-30)	353.9 (-130); 338.8 (- 145); 294.8 (-189); 204.9 (-279)
<i>Detected in synthesized ommatins incubated with β-mercaptoethanol in darkness and in ommochromasome extracts</i>					
β-mercaptoethanol-added xanthommatin (C ₂₂ H ₁₇ N ₃ O ₉ S, 499.45)	11.7	238; 415	499.9 [M+H] ⁺ ; 426.8 (-73)	250.4 [M+2H] ²⁺ ; 227.5 (-23); 218.4 (-32)	482.7 (-17); 464.7 (- 35)
β-mercaptoethanol-added decarboxylated xanthommatin (C ₂₁ H ₁₇ N ₃ O ₇ S, 455.44)	9.1	232; 412	455.9 [M+H] ⁺ ; 420.0 (-36); 382.8 (-73); 343.8 (-112)	228.4 [M+2H] ²⁺ ; 205.4 (-23); 196.5 (-32)	438.8 (-17); 421.0 (- 35); 392.7 (-63)

283 With the aim to produce more ommatins and thus manipulate their molecular structure, we
284 incubated synthesized ommatins for 24 h in MeOH-HCl at 20 °C in darkness (Fig 2C, D). Based on
285 previous studies (Bolognese and Liberatore, 1988), we expected ommatins to get methoxylated,
286 mainly on their carboxylic acid functions. The comparative analysis of Fig 2A, B (2 minutes in
287 MeOH-HCl) and Fig 2C, D (24 h later) highlights different sets of peaks that appeared or disappeared
288 over the 24 h of incubation. Three major newly formed compounds were observed at RT 10.1, 12.6
289 and 13 min corresponding to $[M+H]^+$ at m/z 394, 438 and 452, respectively. We compared the UV and
290 MS characteristics of these compounds with those of xanthommatin and decarboxylated
291 xanthommatin. Absorbance spectra of the five compounds revealed strong similarities, particularly in
292 the visible region (> 400 nm, Fig 3A) suggesting that these three newly formed molecules shared their
293 chromophores with xanthommatin and decarboxylated xanthommatin. Mass spectra of the five
294 compounds also showed strong similarities (Fig 3B). They all experienced an in-source neutral loss of
295 $-17 m/z$ ($-NH_3$) and formed a double-charged molecular ion $[M+2H]^{2+}$. 452 and 394 m/z -associated
296 compounds typically lost 14 units more than xanthommatin and decarboxylated xanthommatin,
297 respectively, during in-source fragmentation. Additionally, their double-charged fragmentations were
298 7 units higher than for xanthommatin and decarboxylated xanthommatin ($= 14/2$; Fig 3B). Overall,
299 gains of 14 m/z in the newly formed compounds compared to xanthommatin and decarboxylated
300 xanthommatin suggested methylation reactions occurring in acidic methanol.

301 Because we did not succeed in purifying each compound to analyze them separately by NMR
302 spectroscopy, we subjected the main $[M+H]^+$ to MS/MS fragmentation and compared it with
303 previously reported fragmentation patterns of kynurenine, 3-hydroxykynurenine, xanthommatin and
304 decarboxylated xanthommatin (Guijas et al., 2018; Panettieri et al., 2018; Reiter et al., 2018; Vazquez
305 et al., 2001; Williams et al., 2016) (<http://metlin.scripps.edu>, METLIN ID: 365). In these molecules,
306 the main ionization site is the amine function of the amino acid branch, which is also the most
307 susceptible to fragmentation. For both xanthommatin and decarboxylated xanthommatin, we observed
308 similar patterns of fragmentation of the amino acid branch with three neutral losses corresponding to -
309 NH_3 ($-17 m/z$), $-CH_5O_2N$ ($-63 m/z$) and $-C_2H_3O_2N$ ($-73 m/z$) (Table 1). Those fragmentations have been

310 reported for these two ommatins (Panettieri et al., 2018; Reiter et al., 2018; Williams et al., 2016), as
311 well as for kynurenines (Vazquez et al., 2001), indicating that they are typical of compounds with a
312 kynurenine-like amino acid chain. Additionally, two neutral losses corresponding to $-\text{CO}_2$ ($-44\ m/z$)
313 and $-\text{CH}_2\text{O}_2$ ($-46\ m/z$) were observed only for xanthommatin (Fig 3C) due to the presence of the
314 carboxyl function on the pyridine ring (Fig 3D). We categorized those predictable MS fragments into
315 different successive fragmentation signatures called F_A to F_E (Table 2) and we used them to assign the
316 structure of unknown ommatins. The fragmentation of $[\text{M}+\text{H}]^+$ $394\ m/z$ showed neutral losses
317 corresponding to $-\text{NH}_3$ ($-17\ m/z = F_A$), $-\text{C}_2\text{H}_7\text{O}_2\text{N}$ ($-77 = -63 -14\ m/z = F_A + F_B + F_C - \text{CH}_2$) and
318 $-\text{C}_3\text{H}_5\text{O}_2\text{N}$ ($-87 = -73 -14\ m/z = F_A + F_B + F_C + F_D - \text{CH}_2$) on the amino acid branch. These results
319 strongly indicated that, in the $394\ m/z$ -associated compound, the carboxyl function of the amino acid
320 branch was methoxylated (α^{11} position). Consequently, this compound was assigned to decarboxylated
321 α^{11} -methoxy-xanthommatin (Fig 3C). Those conclusions are in accordance with the similar absorbance
322 spectra of decarboxylated α^{11} -methoxy-xanthommatin and decarboxylated xanthommatin (Fig 3A), as
323 the amino acid branch is unlikely to act on near-UV and visible wavelength absorptions of the
324 chromophore. The fragmentation of $[\text{M}+\text{H}]^+$ $438\ m/z$ showed the xanthommatin-like neutral losses, -
325 NH_3 ($-17\ m/z = F_A$), $-\text{CH}_5\text{O}_2\text{N}$ ($-63\ m/z = F_A + F_B + F_C$) and $-\text{C}_2\text{H}_3\text{O}_2\text{N}$ ($-73\ m/z = F_A + F_B + F_C + F_D$),
326 highlighting that this compound shared the same unaltered amino acid branch with xanthommatin.
327 However, this compound experienced the neutral loss $-\text{C}_2\text{H}_4\text{O}_2$ ($-60 = -46 -14\ m/z = F_E - \text{CH}_2$) on the
328 pyridine ring instead of $-\text{CH}_2\text{O}_2$ ($-46\ m/z = F_E$) (Fig 3C), which strongly indicated a methoxylation on
329 the pyrido-carboxyl group (α^3 position). This is in accordance with the associated absorbance spectrum
330 being different from that of xanthommatin, which has a carboxylated chromophore (Fig 3A). Hence,
331 we proposed that this compound was α^3 -methoxy-xanthommatin (Fig 3D). The $452\ m/z$ -associated
332 compound showed neutral losses corresponding to $-\text{NH}_3$ ($-17\ m/z = F_A$), $-\text{C}_2\text{H}_7\text{O}_2\text{N}$ ($-77\ m/z = F_A + F_B$
333 $+ F_C - \text{CH}_2$) and $-\text{C}_3\text{H}_5\text{O}_2\text{N}$ ($-87\ m/z = F_A + F_B + F_C + F_D - \text{CH}_2$) on the amino acid branch and $-\text{C}_2\text{H}_4\text{O}_2$
334 ($-60\ m/z = F_D - \text{CH}_2$) on the pyridine ring, which strongly indicated methoxylations on both pyridine
335 ring and amino acid branch in positions α^3 and α^{11} , respectively. This is in accordance with the
336 associated absorbance spectrum being similar to that of α^3 -methoxy-xanthommatin, which has a

337 methoxylated chromophore. Thus, we proposed this compound to be α^3, α^{11} -dimethoxy-xanthommatin
 338 (Fig 3D). Overall, such positions of methoxylation agree well with the reactivity of ommatins in
 339 MeOH-HCl (Bolognese and Liberatore, 1988).

340 Table 2. Diagnostic neutral losses of ommatins.

Annotation	Fragmented structure	Neutral loss	<i>m/z</i> loss
F _A	Amino acid	-NH ₃	-17
F _B	Amino acid	-H ₂ O	-18
F _C	Amino acid	-CO	-28
F _D	Amino acid	-C+2H	-10
F _E	Pyridine ring	-CO ₂ H	-46

341

342 Using the same DAD-MS combination approaches, we annotated other ommatin-like
 343 compounds produced during *in vitro* synthesis and after incubation in MeOH-HCl (Table 1). The 504
 344 and 460 *m/z*-associated compounds differed from xanthommatin and decarboxylated xanthommatin by
 345 80 Da, respectively. The associated double-charged ions $[M+2H]^{2+}$ and $[M-CH_2O_2+2H]^{2+}$ accordingly
 346 differed by 40 *m/z* from those of xanthommatin and decarboxylated xanthommatin, respectively. Their
 347 absorbance spectra were identical to the two ommatins. Their MS and MS/MS spectra revealed
 348 identical losses to xanthommatin and decarboxylated xanthommatin: -NH₃ (-17 *m/z* = F_A), -CH₂O₂ (-
 349 46 *m/z* = F_D), -CH₃O₂N (-63 *m/z* = F_A + F_B + F_C) and -C₂H₃O₂N (-73 *m/z* = F_A + F_B + F_C + F_D; see
 350 Table 2). Furthermore, the $[M+H]^+$ 504 *m/z* experienced the same neutral losses -C₂H₃O₄N (-107 *m/z*)
 351 and -C₃H₅O₄N (-119 *m/z*) than xanthommatin. Alternatively, the $[M+H]^+$ 504 *m/z* experienced a
 352 unique in-source neutral loss of -153 *m/z* that could correspond to -C₂H₃O₅NS or -C₂H₄O₅NP (-73 -80
 353 *m/z*). All those results suggested that the 504 and 460 *m/z*-associated compounds were sulphate or
 354 phosphate esters of xanthommatin and decarboxylated xanthommatin, respectively. This in accordance
 355 with the use of phosphate buffer for the *in vitro* synthesis and of sulfurous acid to precipitate
 356 ommatins. To our knowledge, these two esters have never been described. Finally, during the
 357 incubation in MeOH-HCl, minor ommatin-like compounds (classified as ommatins based on their

358 absorbance and the presence of double-charged ions) were formed and were associated to the 456, 470
359 and 484 m/z (Table 1). The differences of 14 units of their respective molecular ion m/z , as well as
360 their neutral losses in MS/MS being either similar or differing by 14 units, indicated that they were
361 methylated versions of each other. However, due to their very low amounts, we could not
362 unambiguously propose a structure.

363 These results showed that, in storage conditions mimicking extraction procedures with MeOH-
364 HCl, xanthommatin and its decarboxylated form are methoxylated, even in darkness. Those reactions
365 are likely to result from solvent additions with acidified MeOH-HCl (the most efficient solvent for
366 ommatin extraction). To further characterize the importance of those artifactitious reactions, we
367 followed the kinetic of the five ommatins described in Fig 3D in MeOH-HCl at 20 °C and in darkness.

368 *3.2 The ommatin profile is rapidly and readily modified overtime by artifactitious methoxylations* 369 *in acidified methanol*

370 Because absorbance spectra of all five considered compounds did not differ significantly and because
371 some of them were co-eluted (Fig 2), their detection and quantification were performed by MS/MS in
372 multiple reaction monitoring (MRM) mode. MRM conditions were independently optimized for each
373 compound based on the fragmentation of their amino acid branch (Fig S2).

374 The MRM signal of xanthommatin rapidly decreased overtime in a linear fashion, with a near
375 40 % reduction after only one day of incubation (Fig 4A). On the contrary, the MRM kinetics of α^3 -
376 methoxy-xanthommatin had a logarithmic-shape, sharply increasing during the first day before
377 reaching a plateau during the two following days (Fig 4B). Both decarboxylated α^{11} -methoxy-
378 xanthommatin and α^3, α^{11} -dimethoxy-xanthommatin appeared after a few hours of incubation. Their
379 MRM signal then linearly increased overtime (Fig 4C, E). In parallel, the MRM signal of
380 decarboxylated xanthommatin stayed nearly constant, with only a small increase by 1.13 % over the
381 five first hours (Fig 4D). Those results further validate that xanthommatin was readily methoxylated in
382 darkness, primarily in position α^3 . A slower methoxylation on the amino acid branch could account for
383 the delay in the appearance of the two other methoxylated forms. The levels of decarboxylated

384 xanthommatin did not vary much overtime although its methoxycarbonyl ester was produced (Fig 4D,
385 E). This result could be explained by the concomitant and competitive slow decarboxylation of
386 xanthommatin, a reaction that has already been described in MeOH-HCl upon light radiations
387 (Bolognese et al., 1988b).

388 Because we cannot compare MRM signal intensities of different molecules, we took benefit of
389 their similar absorption in the visible region, especially at 414 nm (Fig 3A, Fig S3), to quantify their
390 relative amounts. Although less sensitive and less specific than MRM-based detection, the absorbance
391 at 414 nm strongly indicated that, after only one day of incubation, one third of ommatins was
392 methoxylated (Fig 4F). Most of the methoxylated ommatins accumulated during the first 24 hours (Fig
393 4B). As expected, rates of methoxylation were significantly decreased by incubating synthesized
394 ommatins in MeOH-HCl at -20 °C (Fig S4A, B). After storage of a month at -20 °C, the methoxylated
395 ommatins represented nearly 1.2 % of ommatins (Fig S4C).

396 To conclude, our results showed that decarboxylated xanthommatin was mostly stable in
397 MeOH-HCl. By contrast, xanthommatin was rapidly converted into methoxylated derivatives. Since,
398 MeOH-HCl is the most efficient solvent for ommatin extraction, the conditions for extraction and
399 analysis of ommatins from biological samples should avoid wherever possible the formation of
400 artifactitious methoxylated ommatins.

401 *3.3 UPLC-DAD-MS/MS structural elucidation of uncyclized xanthommatin, the labile* 402 *intermediate in the synthesis of ommatins from 3-hydroxykynurenine*

403 The *in vitro* synthesis of xanthommatin by oxidizing 3-hydroxykynurenine additionally yielded a
404 minor compound at RT 6.7 min. It was characterized by a peak of absorbance at 430 nm and was
405 associated to the 443 *m/z* feature (Fig 2A, B). Upon solubilization in MeOH-HCl, the unidentified
406 compound was labile and disappeared after the 24h-incubation at 20 °C in darkness (Fig 2C, D). A
407 similar 443 *m/z* feature was described two decades ago during oxidations of 3-hydroxykynurenine in
408 various conditions (Iwahashi and Ishii, 1997). Based on its MS spectrum, it was assigned putatively to
409 the 3-hydroxykynurenine dimer called uncyclized xanthommatin. However, there was a lack of

410 analytical evidence to support its structural elucidation. No study has ever since reported the presence
411 of uncyclized xanthommatin, either *in vitro* or *in vivo*. Because this compound could be an important
412 biological intermediate in the formation of ommatins (Bolognese et al., 1988b; Iwahashi and Ishii,
413 1997), we further characterized its structure based on its chemical behavior, absorbance and
414 fragmentation pattern. We note that the apparent lability and the very low amounts of this unidentified
415 product precluded its characterization by NMR spectroscopy.

416 The absorbance and MS kinetics of the unidentified synthesized compound showed that it was
417 very labile (insets of Fig 5A, B). Indeed, we could not detect it after a week of storage at -20 °C
418 anymore. This behavior resembled that of a photosensitive ommatin-like isolated 40 years ago from
419 several invertebrates, which rapidly turned into xanthommatin after extraction (Bolognese and
420 Scherillo, 1974). The absorbance spectrum of this unidentified compound matched almost exactly the
421 UV-Visible spectrum of cinnabaric acid measured in the same conditions (Fig 5C), and both are
422 similar to those reported for actinomycin D and 2-amino-phenoxazin-3-one (Nakazawa et al., 1981).
423 This result indicated that this compound contained the amino-phenoxazinone chromophore rather than
424 the pyrido[3,2-*a*]phenoxazinone scaffold of ommatins or the *ortho*-aminophenol core of 3-
425 hydroxykynurenine. Furthermore, its ionization pattern revealed striking similarities with ommatins.
426 Along with the molecular ion $[M+H]^+$ at 443 *m/z* (corresponding to MW 442 and to the formula
427 $C_{20}H_{18}N_4O_8$), we detected the double-charged ion $[M-NH_3+2H]^{2+}$ at 213.6 *m/z* (Fig 5D). We then
428 targeted the molecular ion for MS/MS to compare the obtained fragments with those reported above
429 (Table 2). If the compound was uncyclized xanthommatin, we predicted that F_A , F_B , F_C and F_D would
430 appear each twice, because uncyclized xanthommatin possesses two 3-hydroxykynurenine-like amino
431 acid chains. Only F_E should be absent, because no aromatic carboxylic acid exist in uncyclized
432 xanthommatin. Indeed, from two MS^2 spectra obtained at different collision energies, we could assign
433 each F_X twice and we did not find any fragmentation event corresponding to F_E . Hence, by starting
434 from the amino-phenoxazinone backbone suggested by the UV-Visible spectrum, the uncyclized form
435 of xanthommatin could be reconstructed after adding each F_{XX} successively (Fig 5F).

436 All these analytical characteristics strongly supported that this labile compound was the
437 phenoxazinone dimer of 3-hydroxykynurenine (Fig 5G), called uncyclized xanthommatin (Figon and
438 Casas, 2019). This structural assignment was further supported by the two following chemical
439 behaviors. First, the oxidation of an *ortho*-aminophenol (here 3-hydroxykynurenine) by potassium
440 ferricyanide is known to induce its dimerization through the loss of six electrons and protons (here $2x$
441 $MW_{3\text{-hydroxykynurenine}} [224 \text{ Da}] - 6 \text{ Da} = MW_{\text{dimer}} [442 \text{ Da}] = MW_{\text{Uncyclized xanthommatin}}$). Second, the
442 spontaneous intramolecular cyclization involving the amine functions of the amino-phenoxazinone
443 core and the closest amino acid branch could explain the lability of uncyclized xanthommatin in cold
444 MeOH-HCl (insets of Fig 5A, B) (Williams et al., 2019a), as well as the formation of a major double-
445 charged ion corresponding to that of the reduced form of xanthommatin (dihydroxanthommatin; Fig
446 5G and Fig S5). The lability of uncyclized xanthommatin questions how we could detect it. We
447 believe there are three main reasons. First, our UHPLC-DAD-MS approach use some of the most
448 sensitive analytical techniques so far. Second, we used rather concentrated samples that allowed us to
449 inject it in sufficient amounts for chromatography, despite the steep decrease in uncyclized
450 xanthommatin during the first hours after extraction. Third, abiotic and biotic factors likely stabilize
451 uncyclized xanthommatin before and during extraction. In particular, we kept all extraction steps at 4
452 °C and in the darkness as much as possible to avoid increased rates of cyclization (Bolognese et al.,
453 1988a; Bolognese and Scherillo, 1974). Furthermore, ommochromes are known to bind to specific
454 proteins, such as ommochrome binding protein and reflectins, which protect them from degradation
455 (Williams et al., 2019b); it is therefore possible that uncyclized xanthommatin is stabilized *in vivo* by
456 binding to proteins. In conclusion, we have now the tools to identify uncyclized xanthommatin in
457 other samples, particularly biological materials.

458 ***3.4 Biological localization of the metabolites from the tryptophan → ommochrome pathway***

459 Using our chemical and analytical knowledge of synthesized ommatins, we reinvestigated the content
460 of housefly eyes in ommochromes and their related metabolites. We chose this species because it is
461 known to accumulate xanthommatin and some metabolites of the kynurenine pathway in its eyes
462 (Linzen, 1974). However, nothing is known about decarboxylated xanthommatin and uncyclized

463 xanthommatin because they were recently described [(Figon and Casas, 2019) and this study], even
464 though the presence of uncyclized xanthommatin has been suspected (Bolognese and Scherillo, 1974).
465 Furthermore, a protocol to extract and purify ommochromasomes from housefly eyes is available
466 (Cölln et al., 1981), thus we can address the question of the localization of the metabolites from the
467 tryptophan→ommochrome pathway. Finally, we designed an extraction protocol in which all steps
468 were performed in darkness, at low temperature and in less than half an hour. In those conditions, we
469 were confident that artifactitious methoxylated ommatins would represent less than one percent of all
470 ommatins and that we could still detect uncyclized xanthommatin.

471 Based on MRM signals, we detected in methanolic extractions of housefly eyes (called crude
472 extracts; Fig 6A) the following metabolites of the tryptophan→ommochrome pathway: tryptophan, 3-
473 hydroxykynurenine, xanthurenic acid, xanthommatin, decarboxylated xanthommatin and uncyclized
474 xanthommatin (Fig 6B, Table 1). We ascertained the identification of uncyclized xanthommatin by
475 acquiring its absorbance, MS and MS/MS spectra in biological samples. They showed the same
476 features as synthesized uncyclized xanthommatin (Fig S6).

477 We then purified ommochromasomes from housefly eyes by a combination of differential
478 centrifugation and ultracentrifugation, and we compared the extracted compounds with those of crude
479 extracts (Fig 6A). The main metabolites of ommochromasomes were xanthommatin and its
480 decarboxylated form (Fig 6D), in accordance to the function of ommochromasomes as ommochrome
481 factories (Figon and Casas, 2019). Based on the absorbance at 414 nm, decarboxylated xanthommatin
482 represented $5.3 \pm 0.1 \%$ (mean \pm SD, $n = 5$) of all ommatins detected in extracts of
483 ommochromasomes. In comparison, decarboxylated ommatins represented $21.5 \pm 0.2 \%$ (mean \pm SD,
484 $n = 10$) of all ommatins synthesized *in vitro*, a percentage four times higher than in methanolic extracts
485 of purified ommochromasomes (Welch two sample *t*-test, $t = 219.99$, $df = 12.499$, $p\text{-value} < 2.2e^{-16}$).
486 Regarding the precursors of ommochromes in housefly eyes, we could only detect tryptophan and 3-
487 hydroxykynurenine but not the intermediary kynurenine. Tryptophan remained undetectable in
488 extracts of ommochromasomes (Fig 6D). Xanthurenic acid, the product of 3-hydroxykynurenine

489 transamination, was particularly present in crude extracts of housefly eyes but much less in
490 ommochromasomes relatively to 3-hydroxykynurenine (Fig 6C vs. Fig 6E). We also detected the
491 uncyclized form of xanthommatin in ommochromasomes (Fig 6D). We calculated an enrichment ratio
492 of 3-hydroxykynurenine compared to either xanthurenic acid or uncyclized xanthommatin in both
493 crude and ommochromasome extracts, allowing a meaningful comparison between xanthurenic acid
494 and uncyclized xanthommatin in the two extracts. The lower this enrichment ratio is, the more
495 xanthurenic acid or uncyclized xanthommatin is present in the extract. We found that xanthurenic acid
496 was more enriched in crude extracts (mean enrichment of 2.1) than in ommochromasomes (mean
497 enrichment of 11; Student's *t*-test, $t = -8.88$, $df = 8$, $p\text{-value} = 2.04e^{-5}$), while uncyclized xanthommatin
498 was more enriched in ommochromasomes (mean enrichment of 6.2) than in crude extracts (mean
499 enrichment of 21; Student's *t*-test, $t = 5.71$, $df = 8$, $p\text{-value} = 0.00045$).

500 We detected in ommochromasomes two minor ommatin-like compounds associated to the
501 molecular ions 500 and 456 *m/z* (Table 1), which co-eluted with xanthommatin and its decarboxylated
502 form, respectively (Fig 6D). Both unknown compounds were undetectable in crude extracts of
503 housefly eyes. Their associated *m/z* features differed from those of xanthommatin and decarboxylated
504 xanthommatin by 76 units, respectively (Table 1). Because the isolation buffer used for
505 ommochromasome purifications contained β -mercaptoethanol (MW 78 Da), we tested whether those
506 unknown ommatins could be produced by incubating synthesized ommatins with β -mercaptoethanol
507 in a water-based buffer. We did find that 456 and 500 *m/z*-associated compounds were rapidly formed
508 in those *in vitro* conditions and that their retention times matched those detected in ommochromasome
509 extracts (Fig S7). Therefore, the 456 and 500 *m/z*-associated ommatins detected in ommochromasome
510 extracts were likely artifacts arising from the purification procedure via the addition of β -
511 mercaptoethanol. These results further demonstrate that ommochromes are likely to be altered during
512 extraction and purification procedures, a chemical behavior that should be controlled by using
513 synthesized ommochromes incubated in similar conditions than biological samples.

514 **4. Discussion**

515 **4.1 UPLC-DAD-MS/MS structural elucidation of new ommatins**

516 Biological ommochromes are difficult compounds to analyze by NMR spectroscopy
517 (Bolognese et al., 1988b). Only xanthommatin, the most common and studied ommochrome, has been
518 successfully subjected to ¹H-NMR (although no ¹³C- and 2D-NMR data exist to date, to the best of our
519 knowledge) (Kumar et al., 2018; Williams et al., 2019a). The NMR-assisted structural elucidation of
520 unknown ommochromes remains therefore extremely challenging and deceptively difficult. To tackle
521 this structural problem, we used a combination of absorption and mass spectroscopies, which offer
522 high sensitivities and orthogonal information, after separation by liquid chromatography. We report
523 here the most comprehensive analytical dataset to date of ommatins, based on their absorbance, mass
524 and tandem mass spectra (Table 1). This dataset allowed us to elucidate with strong confidence the
525 structure of four new ommochromes, including three methoxylated forms and one labile biological
526 intermediate, and to propose structures for eight new other ommatins.

527 Studies reporting the MS/MS spectra of ommatins demonstrated that they primarily fragment
528 on their amino acid chain (Williams et al., 2016) and then on the pyrido-carboxylic acid, if present
529 (Panettieri et al., 2018). We confirmed those results for other ommatins, which indicates that
530 ommatins fragment in a predictable way despite being highly aromatic compounds. We took a step
531 further by positioning methoxylations based on the differences in fragmentation between
532 methoxylated ommatins and (decarboxylated) xanthommatin. Besides, xanthommatin not only formed
533 a 307 *m/z* fragment but also a major 305 *m/z* fragment (Fig 3C; Table 1). This sole fragment was used
534 in a previous study to annotate a putative new ommochrome called (iso-)elymniommatin, an isomer of
535 xanthommatin (Panettieri et al., 2018). Our results prove that MS/MS spectra cannot distinguish (iso-
536)elymniommatin and xanthommatin unambiguously. The use of synthesized ommatins and further
537 experiments are thus needed to verify the existence of (iso-)elymniommatin in butterfly wings.

538 Overall, this analytical dataset will help future studies to identify known biosynthesized and
539 artifactitious ommatins in biological samples, as well as to elucidate the structure of unknown

540 ommatins by analyzing their absorbance and mass spectra in the absence of NMR data. Furthermore, it
541 is now possible to look for uncyclized xanthommatin in a wide variety of species.

542 *4.2 Biological extracts are prone to yield artifactitious ommatins*

543 It has long been reported that ommatins are photosensitive compounds that react with acidified
544 methanol (MeOH-HCl) upon light radiation, leading to their reduction, methylation, methoxylation,
545 decarboxylation and deamination (Bolognese et al., 1988c, 1988d; Bolognese and Liberatore, 1988;
546 Figon and Casas, 2019). Nevertheless, incubating tissues in MeOH-HCl for several hours at room
547 temperature has been commonly used to extract ommatins from biological samples efficiently
548 (Bolognese et al., 1988a; Riou and Christidès, 2010; Zhang et al., 2017). Our results demonstrate that,
549 even in the absence of light radiation, ommatins are readily and rapidly methoxylated by thermal
550 additions of methanol, primarily on the carboxylic acid function of the pyridine ring and secondarily
551 on the amino acid chain (Fig 7). The $[M+H]^+$ 438 m/z of α^3 -methoxy-xanthommatin identified in our
552 study could correspond to the same $[M+H]^+$ previously reported in extracts of butterfly wings
553 (Panettieri et al., 2018). Hence, artifactitious methoxylations during extraction should first be ruled out
554 before assigning methoxylated ommatins to a new biosynthetic pathway. We also show that ommatins
555 react with other extraction buffers since we detected β -mercaptoethanol-added ommatins when
556 synthesized ommatins were incubated in a phosphate buffer containing that reducing agent. Overall,
557 these results emphasize the need to control for potential artifactitious reactions when performing any
558 extraction or purification protocol of biological ommochromes.

559 *4.3 The metabolites of the tryptophan \rightarrow ommochrome pathway in ommochromasomes*

560 It has long been hypothesized that precursors of ommochromes are translocated within
561 ommochromasomes by the transmembrane ABC transporters White and Scarlet (Ewart et al., 1994;
562 Mackenzie et al., 2000). Here, we clearly demonstrate that 3-hydroxykynurenine, but not tryptophan,
563 occurs in ommochromasome fractions of housefly eyes, confirming that 3-hydroxykynurenine is the
564 precursor imported into ommochromasomes by White and Scarlet transporters (Fig 8).

565 Our results confirm that xanthommatin is the main ommatin in ommochromosomes of
566 housefly eyes. We also showed that decarboxylated xanthommatin was present in significant amounts,
567 which could not be solely due to the slow decarboxylation of xanthommatin in MeOH-HCl. This result
568 indicates that both xanthommatin and its decarboxylated form are produced from 3-
569 hydroxykynurenine within ommochromosomes (Fig 8). We also detected xanthurenic acid, the
570 cyclized form of 3-hydroxykynurenine, in housefly eyes. Compared to 3-hydroxykynurenine,
571 xanthurenic acid was present in minute amounts within ommochromosomes. We hypothesize that
572 xanthurenic acid is produced within ommochromosomes via two non-exclusive pathways (Fig 8). The
573 first route is the *in situ* intramolecular cyclization of 3-hydroxykynurenine, which requires a cytosolic
574 transaminase activity (HKT; Fig 8) (Han et al., 2007). The second route is the degradation of
575 xanthommatin that would produce 3-hydroxykynurenine and xanthurenic acid. The phenoxazinone
576 structure of ommatins is indeed known to undergo ring-cleavage, particularly in slightly basic water-
577 based buffers (Butenandt and Schäfer, 1962). Hence, traces of xanthurenic acid might either come
578 from degradation during the purification protocol or from biological changes in ommochromosome
579 conditions (enzymatic activities or basification) leading to the cleavage of xanthommatin. To the best
580 of our knowledge, no biological pathways for the degradation of the pyrido-phenoxazinone structure
581 of ommatins have been described. The detection of xanthurenic acid in ommochromosomes might
582 therefore be the first step towards understanding the *in situ* catabolism of ommatins (Fig 8).

583 Experimental and computational chemists have long hypothesized that the pyrido[3,2-
584 a]phenoxazinone structure of ommatins should be synthesized *in vivo* by the dimerization of 3-
585 hydroxykynurenine and a subsequent spontaneous intramolecular cyclization (Butenandt, 1957;
586 Zhuravlev et al., 2018). However, the associated dimer of 3-hydroxykynurenine, called uncyclized
587 xanthommatin, proved to be difficult to characterize and to isolate from biological samples because of
588 its lability (Bolognese and Scherillo, 1974). In our study, we synthesized uncyclized xanthommatin by
589 the oxidative condensation of 3-hydroxykynurenine with potassium ferricyanide, an oxidant known to
590 form amino-phenoxazinones from *ortho*-aminophenols (Bolognese and Scherillo, 1974). We used a
591 combination of kinetics and analytical spectroscopy (DAD, MS and MS/MS) to confirm the *in vitro*

592 and biological occurrence of uncyclized xanthommatin. Because we detected xanthommatin, its
593 decarboxylated form, their precursor 3-hydroxykynurenine and the intermediary uncyclized
594 xanthommatin in both *in vitro* and biological samples, we argue that the *in vitro* synthesis and the
595 biosynthesis of ommatins proceed through a similar mechanism (compare Fig 7 and Fig 8). An
596 alternative biosynthetic pathway for ommatins has been proposed to occur through the condensation of
597 3-hydroxykynurenine with xanthurenic acid (hypothesis 2, Fig 1B) (Linzen, 1974; Panettieri et al.,
598 2018). Under the hypothesis that 3-hydroxykynurenine and xanthurenic acid condense into
599 xanthommatin, we would expect them to be in similar quantities within ommochromosomes (i.e.
600 enrichment ratio of 1), which was not the case since their concentrations differed by an order of
601 magnitude. On contrary, under the hypothesis that uncyclized xanthommatin is the intermediate form
602 between 3-hydroxykynurenine and xanthommatin, we would expect it to be enriched in
603 ommochromosomes compared to crude extracts, which was the case either. Furthermore, the fact that
604 the unstable uncyclized xanthommatin was more enriched in ommochromosomes than the stable
605 xanthurenic acid indicates that the flux of 3-hydroxykynurenine dimerization is high enough to
606 counterbalance the disappearance of uncyclized xanthommatin by intramolecular cyclization. Thus,
607 uncyclized xanthommatin is unlikely solely a by-product. At the very least, our results show that
608 xanthurenic acid is tightly linked to the ommochrome pathway and therefore cannot be considered as a
609 marker of a distinct biogenic pathway. Lastly, as far as we know, there has been no experimental
610 evidence for the formation of xanthommatin by condensing 3-hydroxykynurenine with xanthurenic
611 acid. In conclusion, the formation of uncyclized xanthommatin by the oxidative dimerization of 3-
612 hydroxykynurenine is likely to be the main biological route for the biosynthesis of ommatins within
613 ommochromosomes (Fig 8).

614 Whether the *in vivo* oxidative dimerization of 3-hydroxykynurenine is catalyzed enzymatically
615 remains a key question in the biogenesis of ommochromes (Figon and Casas, 2019). Theoretical
616 calculations suggested that both enzymatic and non-enzymatic oxidations of 3-hydroxykynurenine
617 would lead to the formation of the phenoxazinone uncyclized xanthommatin (Williams et al., 2019a;
618 Zhuravlev et al., 2018). There was some evidence of a phenoxazinone synthase (PHS) activity

619 associated to purified ommochromosomes of fruitflies (Yamamoto et al., 1976). However, no
620 corresponding PHS enzyme has ever been isolated nor identified in species producing ommochromes
621 (Figon and Casas, 2019). PHS is not the only enzyme capable of forming aminophenoxazinones from
622 *ortho*-aminophenols. Tyrosinase, laccase, peroxidase and catalase can also catalyze these reactions (Le
623 Roes-Hill et al., 2009). Particularly, peroxidase can produce xanthommatin and its decarboxylated
624 form from 3-hydroxykynurenine *in vitro* (Ishii et al., 1992; Iwahashi and Ishii, 1997; Vazquez et al.,
625 2000; Vogliardi et al., 2004), likely through the formation of uncyclized xanthommatin (Iwahashi and
626 Ishii, 1997). This result relates to the long-known fact that insects mutated for the heme peroxidase
627 Cardinal accumulate 3-hydroxykynurenine without forming ommochromes (Howells et al., 1977;
628 Osanai-Futahashi et al., 2016). Hence, our data support the hypothesis that the biosynthesis of
629 ommatins could be catalyzed by a relatively unspecific peroxidase such as Cardinal (Fig 8) (Liu et al.,
630 2017; Osanai-Futahashi et al., 2016), without the requirement of a specialized PHS.

631 *4.4 Uncyclized xanthommatin is a potential key branching point in the biogenesis of ommatins* 632 *and ommins*

633 The relatively recent description of decarboxylated xanthommatin in several species indicates that it is
634 a common biological ommatin (Figon and Casas, 2019). Yet, little is known about how
635 decarboxylation of ommatins proceeds *in vivo*. In this study, we show that decarboxylated
636 xanthommatin is unlikely to arise solely from the artifactitious decarboxylation of xanthommatin in
637 MeOH-HCl, and that the level of decarboxylated xanthommatin is lower in biological extracts (5.3 %)
638 than *in vitro* (21.5 %). Three biological mechanisms could account for the biosynthesis of
639 decarboxylated xanthommatin (Fig 8). (1) The decarboxylation of xanthommatin in water-based
640 environments and upon light radiations possibly accounted for the formation of decarboxylated
641 xanthommatin (Fig 8). Indeed, some aromatic compounds are known to be decarboxylated by the
642 action of water (Mundle and Kluger, 2009), and kynurenic acid, which is structurally related to
643 xanthommatin, is decarboxylated upon light radiations (Zelentsova et al., 2013). (2) Enzymatic and
644 non-enzymatic syntheses of ommatins might differ in their products and exact molecular steps (Ishii et

645 al., 1992; Zhuravlev et al., 2018). Thus, the proposed involvement of the heme peroxidase Cardinal in
646 the biosynthesis of ommatins (Howells et al., 1977) might lead to the natural formation of
647 xanthommatin over its decarboxylated form. (3) Bolognese and colleagues proposed that
648 decarboxylation happens by a rearrangement of protons, consecutively to the intramolecular
649 cyclization of uncyclized xanthommatin (Bolognese et al., 1988b). Such mechanism has been well
650 described for the biogenesis of eumelanin monomers, in which the non-decarboxylative rearrangement
651 of dopachrome is favored by the dopachrome tautomerase (Solano et al., 1996). Hence, this analogy
652 raises the intriguing possibility that a tautomerase might catalyze the formation of xanthommatin from
653 uncyclized xanthommatin (Fig 8), thereby controlling the relative content of decarboxylated
654 xanthommatin in ommochromosomes, which is known to vary among species, individuals and
655 chromatophores (Futahashi et al., 2012; Williams et al., 2016; Zhang et al., 2017). Why
656 decarboxylated xanthommatin levels depend on the biological context may rely on its biological
657 functions, which we now discuss.

658 Few studies have addressed the biological function of decarboxylated xanthommatin. Its ratio
659 to xanthommatin is known to vary among species and individuals (Futahashi et al., 2012; Williams et
660 al., 2016). In cephalopods, the ratio of xanthommatin to its decarboxylated form within a
661 chromatophore has been suggested to determine its color, ranging from yellow to purple (Williams et
662 al., 2016). However, our absorbance data do not support this hypothesis because the experimental
663 absorbance spectrum of decarboxylated xanthommatin was not different from that of xanthommatin in
664 the visible region. Moreover, purple colors are produced by chromophores that absorb wavelengths
665 around 520 nm, which has not been described for any ommatin in contrast to ommins (Figon and
666 Casas, 2019). Another study focusing on the quantum chemistry of pirenoxine, a xanthommatin-like
667 drug, proposed that the carboxylic acid function present on the pyrido[3,2-*a*]phenoxazinone of
668 pirenoxine could enhance its binding to divalent cations (Liao et al., 2011). This is coherent with the
669 fact that ommochromosomes accumulate and store cations, such as Ca²⁺ and Mg²⁺ (Gribakin et al.,
670 1987; Ukhanov, 1991). Thus, favoring xanthommatin over its decarboxylated form *in vivo* might
671 enhance the storage of metals in ommochromosomes, as proposed for eumelanins that contain high

672 proportions of the carboxylated monomers DHICA (Hong and Simon, 2007). To which extent the
673 binding of metals modifies the physical and chemical properties of ommatins, therefore their
674 biological roles, remains to be determined.

675 How ommatins and ommins, the two most abundant families of ommochromes, are
676 biochemically connected to each other is still a mystery (Figon and Casas, 2019). Purple ommins have
677 higher molecular weights than ommatins and derive from both 3-hydroxykynurenine and
678 cysteine/methionine, the latter providing sulfur to the phenothiazine ring of ommins (Linzen, 1974;
679 Needham, 1974). The best-known ommin is called ommin A, whose structure was proposed to be a
680 trimer of 3-hydroxykynurenine in which one of the phenoxazine ring is replaced by phenothiazine (Fig
681 8) (Needham, 1974). Since the pyrido[3,2-*a*]phenoxazinone cannot be reopened to an amino-
682 phenoxazinone in anyway (Bolognese and Liberatore, 1988), it is unlikely that the biosynthesis of
683 ommins is a side-branch of ommatins. Thus, the biochemical relationship between ommatins and
684 ommins should be found upstream in the biosynthetic pathway of ommochromes. Older genetic and
685 chemical studies demonstrated that ommins and ommatins share the kynurenine pathway and Linzen
686 proposed that the ratio of xanthommatin to ommins could depend on the level of methionine-derived
687 precursors (Linzen, 1974). The distinct structure of uncyclized xanthommatin raises the interesting
688 hypothesis that uncyclized xanthommatin is the elusive intermediate between the *ortho*-aminophenol
689 structure of 3-hydroxykynurenine, the pyrido-phenoxazinone chromophore of xanthommatin and the
690 phenoxazine-phenothiazine structure of ommins. We propose that the biosynthesis of ommins first
691 proceeds with the dimerization of 3-hydroxykynurenine into uncyclized xanthommatin, then with the
692 stabilization of its amino acid chain to avoid a spontaneous intramolecular cyclization, and finally with
693 the condensation with a sulfur-containing compound derived from methionine/cysteine (Fig 8).
694 Although this mechanism is hypothetical at this stage, it can explain two apparently unrelated
695 observations. First, it clarifies the reason why *cardinal* mutants of insects, which lack the heme
696 peroxidase Cardinal that possibly catalyzes the formation of uncyclized xanthommatin, lack both
697 ommatins and ommins, and accumulate 3-hydroxykynurenine (Howells et al., 1977; Osanai-Futahashi
698 et al., 2016). Second, it could explain how a single cephalopod chromatophore can change its color

699 from yellow (ommatins) to purple (ommins) across its lifetime (Reiter et al., 2018). The biochemical
700 mechanism might be analogous to the casing model of melanins (Ito and Wakamatsu, 2008), in which
701 pheomelanins and eumelanins (in this case ommins and ommatins, respectively) are produced
702 sequentially from the same precursors (uncyclized xanthommatin) through changes in sulfur
703 (methionine/cysteine) availability within melanosomes (ommochromosomes).

704 Overall, uncyclized xanthommatin appears as a key metabolite in the ommochrome pathway
705 by leading to either ommatins, decarboxylated ommatins or ommins (Fig 8). Therefore, the formation
706 of uncyclized xanthommatin might represent a key step in the divergence between the post-kynurenine
707 pathways of vertebrates and invertebrates, as well as in the structural diversification of ommochromes
708 in phylogenetically-distant invertebrates.

709 5. Acknowledgments

710 We thank Kévin Billet, Cédric Delevoye and Emmanuel Gaquerel for fruitful discussions. We are
711 grateful to Antoine Touzé for his technical assistance and for access to the ultracentrifuge. We thank
712 Rustem Uzbekov for providing the electron micrograph. The ENS de Lyon is thanked for financial
713 support (to F. F.). This study formed part of the doctoral dissertation of F. F. under the supervision of
714 J. C.

715 **Conflict of interest:** The authors declare that they have no conflicts of interest with the contents of
716 this article.

717 6. References

- 718 Bolognese, A., Correale, G., Manfra, M., Lavecchia, A., Mazzoni, O., Novellino, E., Barone, V., Pani,
719 A., Tramontano, E., La Colla, P., Murgioni, C., Serra, I., Setzu, G., Loddo, R., 2002.
720 Antitumor Agents. 1. Synthesis, Biological Evaluation, and Molecular Modeling of 5 *H* -
721 Pyrido[3,2- *a*]phenoxazin-5-one, a Compound with Potent Antiproliferative Activity. *Journal*
722 *of Medicinal Chemistry* 45, 5205–5216. <https://doi.org/10.1021/jm020913z>
723 Bolognese, A., Liberatore, R., 1988. Photochemistry of ommochrome pigments. *Journal of*
724 *Heterocyclic Chemistry* 25, 1243–1246. <https://doi.org/10.1002/jhet.5570250438>
725 Bolognese, A., Liberatore, R., Piscitelli, C., Scherillo, G., 1988a. A Light-Sensitive Yellow
726 Ommochrome Pigment From the House Fly. *Pigment Cell Research* 1, 375–378.
727 <https://doi.org/10.1111/j.1600-0749.1988.tb00137.x>

- 728 Bolognese, A., Liberatore, R., Riente, G., Scherillo, G., 1988b. Oxidation of 3-hydroxykynurenine. A
729 reexamination. *Journal of Heterocyclic Chemistry* 25, 1247–1250.
730 <https://doi.org/10.1002/jhet.5570250439>
- 731 Bolognese, A., Liberatore, R., Scherillo, G., 1988c. Photochemistry of ommochromes and related
732 compounds. *Journal of Heterocyclic Chemistry* 25, 979–983.
733 <https://doi.org/10.1002/jhet.5570250353>
- 734 Bolognese, A., Liberatore, R., Scherillo, G., 1988d. Photochemistry of ommochromes and related
735 compounds. Part II. *Journal of Heterocyclic Chemistry* 25, 1251–1254.
736 <https://doi.org/10.1002/jhet.5570250440>
- 737 Bolognese, A., Scherillo, G., 1974. Occurrence and characterization of a labile xanthommatin
738 precursor in some invertebrates. *Experientia* 30, 225–226.
739 <https://doi.org/10.1007/BF01934793>
- 740 Butenandt, A., 1957. Über Ommochrome, eine Klasse natürlicher Phenoxazon-Farbstoffe.
741 *Angewandte Chemie* 69, 16–23. <https://doi.org/10.1002/ange.19570690104>
- 742 Butenandt, A., Schäfer, W., 1962. Ommochromes, in: *Recent Progress in the Chemistry of Natural and*
743 *Synthetic Colouring Matters and Related Fields*. Academic Press, New York, NY, pp. 13–33.
- 744 Butenandt, A., Schiedt, U., Biekert, E., 1954. Über Ommochrome, III. Mitteilung: Synthese des
745 Xanthommatins. *Justus Liebigs Annalen der Chemie* 588, 106–116.
- 746 Cölln, K., Hedemann, R., Ojijo, E., 1981. A method for the isolation of ommochrome-containing
747 granules from insect eyes. *Experientia* 37, 44–46.
- 748 Crescenzi, O., Correale, G., Bolognese, A., Piscopo, V., Parrilli, M., Barone, V., 2004. Observed and
749 calculated ¹H- and ¹³C-NMR chemical shifts of substituted 5H-pyrido[3,2-a]- and 5H-
750 pyrido[2,3-a]phenoxazin-5-ones and of some 3H-phenoxazin-3-one derivatives. *Org. Biomol.*
751 *Chem.* 2, 1577–1581. <https://doi.org/10.1039/B401147C>
- 752 Croucher, P.J., Brewer, M.S., Winchell, C.J., Oxford, G.S., Gillespie, R.G., 2013. De novo
753 characterization of the gene-rich transcriptomes of two color-polymorphic spiders, *Theridion*
754 *grallator* and *T. californicum* (Araneae: Theridiidae), with special reference to pigment genes.
755 *BMC Genomics* 14, 862. <https://doi.org/10.1186/1471-2164-14-862>
- 756 Ewart, G.D., Cannell, D., Cox, G.B., Howells, A.J., 1994. Mutational analysis of the traffic ATPase
757 (ABC) transporters involved in uptake of eye pigment precursors in *Drosophila melanogaster*.
758 Implications for structure-function relationships. *J. Biol. Chem.* 269, 10370–10377.
- 759 Figon, F., Casas, J., 2019. Ommochromes in invertebrates: biochemistry and cell biology. *Biological*
760 *Reviews* 94, 156–183. <https://doi.org/10.1111/brv.12441>
- 761 Futahashi, R., Kurita, R., Mano, H., Fukatsu, T., 2012. Redox alters yellow dragonflies into red.
762 *Proceedings of the National Academy of Sciences* 109, 12626–12631.
763 <https://doi.org/10.1073/pnas.1207114109>
- 764 Gribakin, F.G., Burovina, I.V., Chesnokova, Y.G., Natochin, Y.V., Shakmatova, Y.I., Ukhanov, K.Y.,
765 Woyke, E., 1987. Reduced magnesium content in non-pigmented eyes of the honey bee (*Apis*
766 *mellifera* L.). *Comparative Biochemistry and Physiology Part A: Physiology* 86, 689–692.
- 767 Guijas, C., Montenegro-Burke, J.R., Domingo-Almenara, X., Palermo, A., Warth, B., Hermann, G.,
768 Koellensperger, G., Huan, T., Uritboonthai, W., Aisporna, A.E., Wolan, D.W., Spilker, M.E.,
769 Benton, H.P., Siuzdak, G., 2018. METLIN: A Technology Platform for Identifying Knowns
770 and Unknowns. *Analytical Chemistry* 90, 3156–3164.
771 <https://doi.org/10.1021/acs.analchem.7b04424>
- 772 Han, Q., Beerntsen, B.T., Li, J., 2007. The tryptophan oxidation pathway in mosquitoes with emphasis
773 on xanthurenic acid biosynthesis. *Journal of Insect Physiology* 53, 254–263.
774 <https://doi.org/10.1016/j.jinsphys.2006.09.004>
- 775 Hong, L., Simon, J.D., 2007. Current Understanding of the Binding Sites, Capacity, Affinity, and
776 Biological Significance of Metals in Melanin. *The Journal of Physical Chemistry B* 111,
777 7938–7947. <https://doi.org/10.1021/jp071439h>
- 778 Hori, M., Riddiford, L.M., 1981. Isolation of ommochromes and 3-hydroxykynurenine from the
779 tobacco hornworm, *Manduca sexta*. *Insect Biochemistry* 11, 507–513.
780 [https://doi.org/10.1016/0020-1790\(81\)90018-4](https://doi.org/10.1016/0020-1790(81)90018-4)

- 781 Howells, A.J., Summers, K.M., Ryall, R.L., 1977. Developmental patterns of 3-hydroxykynurenine
782 accumulation in white and various other eye color mutants of *Drosophila melanogaster*.
783 *Biochem. Genet.* 15, 1049–1059.
- 784 Ishii, T., Iwahashi, H., Sugata, R., Kido, R., 1992. Formation of hydroxanthommatin-derived radical in
785 the oxidation of 3-hydroxykynurenine. *Archives of biochemistry and biophysics* 294, 616–
786 622.
- 787 Ito, S., Wakamatsu, K., 2008. Chemistry of Mixed Melanogenesis—Pivotal Roles of Dopaquinone.
788 *Photochemistry and Photobiology* 84, 582–592. [https://doi.org/10.1111/j.1751-
789 1097.2007.00238.x](https://doi.org/10.1111/j.1751-1097.2007.00238.x)
- 790 Iwahashi, H., Ishii, T., 1997. Detection of the oxidative products of 3-hydroxykynurenine using high-
791 performance liquid chromatography–electrochemical detection–ultraviolet absorption
792 detection–electron spin resonance spectrometry and high-performance liquid
793 chromatography–electrochemical detection–ultraviolet absorption detection–mass
794 spectrometry. *Journal of Chromatography A* 773, 23–31.
- 795 Kumar, A., Williams, T.L., Martin, C.A., Figueroa-Navedo, A.M., Deravi, L.F., 2018. Xanthommatin-
796 Based Electrochromic Displays Inspired by Nature. *ACS Applied Materials & Interfaces*.
797 <https://doi.org/10.1021/acsami.8b14123>
- 798 Le Roes-Hill, M., Goodwin, C., Burton, S., 2009. Phenoxazinone synthase: what's in a name? *Trends*
799 *in Biotechnology* 27, 248–258. <https://doi.org/10.1016/j.tibtech.2009.01.001>
- 800 Liao, J.-H., Chen, C.-S., Hu, C.-C., Chen, W.-T., Wang, S.-P., Lin, I.-L., Huang, Y.-H., Tsai, M.-H.,
801 Wu, T.-H., Huang, F.-Y., Wu, S.-H., 2011. Ditopic Complexation of Selenite Anions or
802 Calcium Cations by Pirenoxine: An Implication for Anti-Cataractogenesis. *Inorganic*
803 *Chemistry* 50, 365–377. <https://doi.org/10.1021/ic102151p>
- 804 Linzen, B., 1974. The Tryptophan → Ommochrome Pathway in Insects, in: Treherne, J.E., Berridge,
805 M.J., Wigglesworth, V.B. (Eds.), *Advances in Insect Physiology*. Elsevier, Academic Press,
806 pp. 117–246.
- 807 Liu, S.-H., Luo, J., Yang, B.-J., Wang, A.-Y., Tang, J., 2017. *karmoisin* and *cardinal* ortholog genes
808 participate in the ommochrome synthesis of *Nilaparvata lugens* (Hemiptera: Delphacidae).
809 *Insect Science*. <https://doi.org/10.1111/1744-7917.12501>
- 810 Mackenzie, S.M., Howells, A.J., Cox, G.B., Ewart, G.D., 2000. Sub-cellular localisation of the
811 white/scarlet ABC transporter to pigment granule membranes within the compound eye of
812 *Drosophila melanogaster*. *Genetica* 108, 239–252.
- 813 Mundle, S.O.C., Kluger, R., 2009. Decarboxylation via Addition of Water to a Carboxyl Group: Acid
814 Catalysis of Pyrrole-2-Carboxylic Acid. *Journal of the American Chemical Society* 131,
815 11674–11675. <https://doi.org/10.1021/ja905196n>
- 816 Nakazawa, H., Chou, F.E., Andrews, P.A., Bachur, N.R., 1981. Chemical reduction of actinomycin D
817 and phenoxazone analog to free radicals. *J. Org. Chem.* 46, 1493–1496.
818 <https://doi.org/10.1021/jo00320a054>
- 819 Needham, A.E., 1974. The significance of zochromes, *Zoophysiology and ecology*. Springer-Verlag,
820 Berlin, Heidelberg, New York.
- 821 Osanai-Futahashi, M., Tatematsu, K., Futahashi, R., Narukawa, J., Takasu, Y., Kayukawa, T.,
822 Shinoda, T., Ishige, T., Yajima, S., Tamura, T., Yamamoto, K., Sezutsu, H., 2016. Positional
823 cloning of a *Bombyx* pink-eyed white egg locus reveals the major role of cardinal in
824 ommochrome synthesis. *Heredity* 116, 135–145. <https://doi.org/10.1038/hdy.2015.74>
- 825 Panettieri, S., Gjinaj, E., John, G., Lohman, D.J., 2018. Different ommochrome pigment mixtures
826 enable sexually dimorphic Batesian mimicry in disjunct populations of the common palmfly
827 butterfly, *Elymnias hypermnestra*. *PLOS ONE* 13, e0202465.
828 <https://doi.org/10.1371/journal.pone.0202465>
- 829 Parrilli, M., Bolognese, A., 1992. 1H and 13C Chemical Shift Data of Some Ommochrome Models:
830 Substituted Benzo[3,2-a]-5H-phenoxazin-5-one. *Heterocycles* 34, 1829.
831 <https://doi.org/10.3987/COM-92-6106>
- 832 Reiter, S., Hülsdunk, P., Woo, T., Lauterbach, M.A., Eberle, J.S., Akay, L.A., Longo, A., Meier-
833 Credo, J., Kretschmer, F., Langer, J.D., Kaschube, M., Laurent, G., 2018. Elucidating the

- 834 control and development of skin patterning in cuttlefish. *Nature* 562, 361–366.
 835 <https://doi.org/10.1038/s41586-018-0591-3>
- 836 Riddiford, L.M., Ajami, A.M., 1971. Identification of an ommochrome in the eyes and nervous
 837 systems of saturniid moths. *Biochemistry* 10, 1451–1455.
 838 <https://doi.org/10.1021/bi00784a028>
- 839 Riou, M., Christidès, J.-P., 2010. Cryptic Color Change in a Crab Spider (*Misumena vatia*):
 840 Identification and Quantification of Precursors and Ommochrome Pigments by HPLC. *Journal*
 841 *of Chemical Ecology* 36, 412–423. <https://doi.org/10.1007/s10886-010-9765-7>
- 842 Solano, F., Jiménez-Cervantes, C., Martínez-Liarte, J.H., García-Borrón, J.C., Jara, J.R., Lozano,
 843 J.A., 1996. Molecular mechanism for catalysis by a new zinc-enzyme, dopachrome
 844 tautomerase. *Biochemical Journal* 313, 447–453. <https://doi.org/10.1042/bj3130447>
- 845 Stubenhaus, B.M., Dustin, J.P., Neverett, E.R., Beaudry, M.S., Nadeau, L.E., Burk-McCoy, E., He, X.,
 846 Pearson, B.J., Pellettieri, J., 2016. Light-induced depigmentation in planarians models the
 847 pathophysiology of acute porphyrias. *eLife* 5, e14175.
- 848 Ukhanov, K.Y., 1991. Ommochrome pigment granules: A calcium reservoir in the dipteran eyes.
 849 *Comparative Biochemistry and Physiology Part A: Physiology* 98, 9–16.
 850 [https://doi.org/10.1016/0300-9629\(91\)90569-X](https://doi.org/10.1016/0300-9629(91)90569-X)
- 851 Vazquez, S., Garner, B., Sheil, M.M., Truscott, R.J., 2000. Characterisation of the major autoxidation
 852 products of 3-hydroxykynurenine under physiological conditions. *Free radical research* 32,
 853 11–23.
- 854 Vazquez, S., Truscott, R.J.W., O’Hair, R.A.J., Weimann, A., Sheil, M.M., 2001. A study of
 855 kynurenine fragmentation using electrospray tandem mass spectrometry. *Journal of the*
 856 *American Society for Mass Spectrometry* 12, 786–794. [https://doi.org/10.1016/S1044-](https://doi.org/10.1016/S1044-0305(01)00255-0)
 857 [0305\(01\)00255-0](https://doi.org/10.1016/S1044-0305(01)00255-0)
- 858 Vogliardi, S., Bertazzo, A., Comai, S., Costa, C.V.L., Allegri, G., Seraglia, R., Traldi, P., 2004. An
 859 investigation on the role of 3-hydroxykynurenine in pigment formation by matrix-assisted
 860 laser desorption/ionization mass spectrometry. *Rapid Communications in Mass Spectrometry*
 861 18, 1413–1420. <https://doi.org/10.1002/rcm.1497>
- 862 Williams, T.L., DiBona, C.W., Dinneen, S.R., Jones Labadie, S.F., Chu, F., Deravi, L.F., 2016.
 863 Contributions of Phenoxazine-Based Pigments to the Structure and Function of
 864 Nanostructured Granules in Squid Chromatophores. *Langmuir* 32, 3754–3759.
 865 <https://doi.org/10.1021/acs.langmuir.6b00243>
- 866 Williams, T.L., Lopez, S.A., Deravi, L.F., 2019a. A Sustainable Route To Synthesize the
 867 Xanthommatin Biochrome via an Electro-catalyzed Oxidation of Tryptophan Metabolites.
 868 *ACS Sustainable Chem. Eng.* [acssuschemeng.9b01144](https://doi.org/10.1021/acssuschemeng.9b01144).
 869 <https://doi.org/10.1021/acssuschemeng.9b01144>
- 870 Williams, T.L., Senft, S.L., Yeo, J., Martín-Martínez, F.J., Kuzirian, A.M., Martin, C.A., DiBona,
 871 C.W., Chen, C.-T., Dinneen, S.R., Nguyen, H.T., Gomes, C.M., Rosenthal, J.J.C., MacManes,
 872 M.D., Chu, F., Buehler, M.J., Hanlon, R.T., Deravi, L.F., 2019b. Dynamic pigmentary and
 873 structural coloration within cephalopod chromatophore organs. *Nature Communications* 10.
 874 <https://doi.org/10.1038/s41467-019-08891-x>
- 875 Yamamoto, M., Howells, A.J., Ryall, R.L., 1976. The ommochrome biosynthetic pathway in
 876 *Drosophila melanogaster*: The head particulate phenoxazinone synthase and the
 877 developmental onset of xanthommatin synthesis. *Biochemical Genetics* 14, 1077–1090.
 878 <https://doi.org/10.1007/BF00485139>
- 879 Zelentsova, E.A., Sherin, P.S., Snytnikova, O.A., Kaptein, R., Vauthey, E., Tsentalovich, Y.P., 2013.
 880 Photochemistry of aqueous solutions of kynurenic acid and kynurenine yellow. *Photochem.*
 881 *Photobiol. Sci.* 12, 546–558. <https://doi.org/10.1039/C2PP25357G>
- 882 Zhang, H., Lin, Y., Shen, G., Tan, X., Lei, C., Long, W., Liu, H., Zhang, Y., Xu, Y., Wu, J., Gu, J.,
 883 Xia, Q., Zhao, P., 2017. Pigmentary analysis of eggs of the silkworm *Bombyx mori*. *Journal*
 884 *of Insect Physiology* 101, 142–150. <https://doi.org/10.1016/j.jinsphys.2017.07.013>
- 885 Zhuravlev, A.V., Vetrovoy, O.V., Savvateeva-Popova, E.V., 2018. Enzymatic and non-enzymatic
 886 pathways of kynurenines’ dimerization: the molecular factors for oxidative stress

887 development. PLOS Computational Biology 14, e1006672.
888 <https://doi.org/10.1371/journal.pcbi.1006672>
889

890 **Legends**

891 **Fig 1. Current knowledge of the tryptophan→ommochrome pathway of invertebrates.** A) Main chemical structures and
892 chromophores of the tryptophan→ommochrome pathway. Numbering of ommatins used in this study is indicated on the
893 structure of xanthommatin. B) Kynurenine and ommochrome pathways form the early and late steps of the
894 tryptophan→ommochrome pathway, respectively. Ommatins are possibly biosynthesized via two routes: (1) the dimerization
895 of 3-hydroxykynurenine into the intermediary uncyclized xanthommatin, or (2) the direct condensation of 3-
896 hydroxykynurenine with its cyclized form, xanthurenic acid. Ommatin and ommin pathways share 3-hydroxykynurenine as a
897 precursor, but at which step they diverge is not known. Dashed arrows, steps for which we lack clear biological evidence.
898 HKT, 3-hydroxykynurenine transaminase. KFase, kynurenine formamidase. KMO, kynurenine 3-monooxygenase. Ox.,
899 oxidation. Red., reduction. TDO, tryptophan 2,3-dioxygenase.

900 **Fig 2. Chromatographic profiles of synthesized xanthommatin before and after storage in acidified methanol.**
901 Xanthommatin was synthesized by oxidizing 3-hydroxykynurenine with potassium ferricyanide. **(A-B)** The ommatin solution
902 was subjected to liquid chromatography (LC) two minutes after solubilization in methanol acidified with 0.5 % HCl (MeOH-
903 HCl). The eluted compounds were detected by their absorbance at 440 and 430 nm (A). The main molecular ions
904 (electrospray ionization in positive mode) associated to each peak were monitored by a triple quadrupole mass spectrometer
905 running in single ion reaction (SIR) mode (B). **(C-D)** The same ommatin solution was left for 24 hours at 20 °C in complete
906 darkness. Compounds were separated by LC and detected using the same absorbance (A) and MS modalities (B) as described
907 above.

908 **Fig 3. Absorbance- and mass spectrometry-assisted elucidation of the structure of the five major ommatins detected**
909 **after incubation in acidified methanol.** Ommatins incubated for 24 hours in acidified methanol were analysed by liquid
910 chromatography coupled to a photodiode-array detector and a triple quadrupole mass spectrometer. (A) Absorbance spectra.
911 For each metabolite, absorbance values were reported as percentages of the maximum absorbance value recorded in the range
912 of 200 to 500 nm. Major and minor absorbance peaks are indicated in black and grey fonts, respectively. (B) Mass spectra
913 showing molecular ions and in-source fragments. Black fonts, monocharged ions. Blue fonts, double-charged molecular ions.
914 (C) Tandem mass (MS/MS) spectra of molecular ions obtained by collision-induced dissociation with argon. Black
915 diamonds, $[M+H]^+$ m/z . Green fonts, fragmentations of the amino acid chain. Purple fonts, fragmentations of the pyridine
916 ring are indicated. (D) Elucidated structures of the five ommatins. MS/MS fragmentations are reported in green and purple
917 like in panel C. Black asterisk, main charged basic site. Blue asterisks, potential charged basic sites of the double-charged
918 molecular ions.

919 **Fig 4. Alterations of synthesized ommatins in acidified methanol at 20 °C in darkness.** Synthesized ommatins were
920 solubilized in methanol acidified with 0.5 % HCl (MeOH-HCl) and stored for up to three days at 20 °C and in complete

921 darkness. **(A-E)** Kinetics of alterations were followed by multiple reaction monitoring (MRM) mode of xanthommatin (A),
 922 α^3 -methoxy-xanthommatin (B), α^3, α^{11} -dimethoxy-xanthommatin (C), decarboxylated xanthommatin (D) and decarboxylated
 923 α^{11} -xanthommatin (E). Values are mean \pm SD of four to five samples. (A) Linear regression ($R^2 = 0.96$, $F = 813.5$, $df = 1$ and
 924 32, p -value $< 2.2e-16$). (B) Linear regression with log-scaled time ($R^2 = 0.83$, $F = 159.8$, $df = 1$ and 32, p -value = $5.5e-14$).
 925 (C) Linear regression ($R^2 = 0.98$, $F = 1665$, $df = 1$ and 32, p -value $< 2.2e-16$). (D) Linear regression with log-scaled time (R^2
 926 = 0.35, $F = 17.16$, $df = 1$ and 32, p -value = 0.00023). (E) Linear regression ($R^2 = 0.95$, $F = 651.2$, $df = 1$ and 32, p -value $<$
 927 $2.2e-16$). **(F)** Relative quantifications of methoxylated ommatins compared to unaltered ones (i.e. xanthommatin and
 928 decarboxylated xanthommatin) were performed by measuring the absorbance of ommatins at 414 nm for each time point.
 929 Values are mean \pm SD of five samples. Different letters indicate statistical differences (Kruskal-Wallis rank sum test: $\chi^2 =$
 930 17.857, $df = 3$, p -value = 0.00047; pairwise comparisons using Wilcoxon rank sum test and Holm adjustment: p -values $<$
 931 0.05).

932 **Fig 5. Structural elucidation of uncyclized xanthommatin, the labile intermediate in the synthesis of xanthommatin.**

933 **(A-B)** Chromatographic peaks (absorbance at 430 nm [A] and $[M+H]^+$ 443 m/z recorded in single ion reaction [SIR] mode
 934 [B]) corresponding to the labile ommatin-like compound detected in in vitro synthesis of xanthommatin by the oxidation of
 935 3-hydroxykynurenine with $Fe(CN)_6^{3-}$. Insets show the decay of chromatographic peaks during storage in methanol acidified
 936 with 0.5 % HCl at $-20^\circ C$ in darkness. Values are mean \pm SD of five samples. (A) Linear regression with log-scaled time (R^2
 937 = 0.75, $F = 131.4$, $df = 1$ and 43, p -value = $1.2e-14$). (B) Linear regression with log-scaled time ($R^2 = 0.72$, $F = 111.5$, $df = 1$
 938 and 43, p -value = $1.6e-13$). **(C)** Absorbance spectra. Solid line, labile ommatin-like compound. Dashed line, the
 939 aminophenoxazinone cinnabarinic acid. **(D)** Mass spectrum showing molecular ions and in-source fragments. Black fonts,
 940 monocharged ions. Blue font, double-charged ion. **(E-F)** Tandem mass spectra of the molecular ion obtained by collision-
 941 induced dissociation with argon at collision energies of 20 eV (E) and 30 eV (F). Fragmentations were classified in four types
 942 (F_A to F_D) that occurred twice (F_{X1} and F_{X2}). Black diamonds, $[M+H]^+$ m/z . **(G)** Evidence for the structural elucidation of
 943 uncyclized xanthommatin. Colors of the MS/MS fragmentation pattern correspond to those in panels D-F. Black asterisks,
 944 potential charged basic sites.

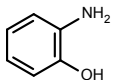
945 **Fig 6. Biological localization of uncyclized xanthommatin and tryptophan \rightarrow ommochrome metabolites from housefly**

946 **eyes. (A)** Overview of the purification and extraction protocols of ommochromes from housefly eyes. **(B)** Chromatographic
 947 profile in Multiple Reaction Monitoring (MRM) mode of the six main metabolites of the tryptophan \rightarrow ommochrome pathway
 948 detected in acidified methanol (MeOH-HCl) extracts of housefly eyes (crude extracts). DcXantho, decarboxylated
 949 xanthommatin, 3-OHK, 3-hydroxykynurenine, Trp, tryptophan, UncXantho, uncyclized xanthommatin. Xantho,
 950 xanthommatin. XA, xanthurenic acid. **(C)** Five μL of crude extract were injected in the chromatographic system and absolute
 951 quantifications of tryptophan, xanthurenic acid, 3-hydroxykynurenine and uncyclized xanthommatin were performed based
 952 on available standards (uncyclized xanthommatin levels are expressed as cinnabarinic acid equivalents). Open circles,

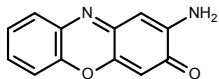
953 measures of five independent extracts. Filled circles and error bars, means \pm SD of five samples. Ratios of 3-
954 hydroxykynurenine to xanthurenic acid and to uncyclized xanthommatin are shown (mean \pm SD, N = 5). **(D-E)** Same as
955 panels B (D) and C (E) but for MeOH-HCl extracts of purified ommochromosomes from housefly eyes. The tryptophan
956 signal was below the signal-to-noise ratio. Statistical differences (p-value < 0.05) between ratios within panels (paired *t*-test)
957 and between panels (unpaired *t*-test) are indicated by different letters and capitals, respectively. N.D., not detected. See
958 Supplemental File S2 for information on statistical analyses. Photograph credits: (A) Sanjay Acharya (CC BY SA).

959 **Fig 7. *In vitro* formation and alteration of ommatins.** Oxidative condensation of the *ortho*-aminophenol 3-
960 hydroxykynurenine proceeds through the loss of six electrons, leading to the formation of the amino-phenoxazinone
961 uncyclized xanthommatin. Uncyclized xanthommatin then rapidly undergoes intramolecular cyclization and oxidation,
962 forming the two pyrido[3,2-*a*]phenoxazinone xanthommatin and decarboxylated xanthommatin. Decarboxylated
963 xanthommatin could also be produced from the direct decarboxylation of xanthommatin. In acidified conditions, ommatins
964 readily undergo thermal additions of methanol, which leads to their methoxylation. In solution, uncyclized xanthommatin
965 also decays by intramolecular cyclization and xanthommatin slowly decarboxylates. Relative sizes of arrows are indicative of
966 reaction rates.

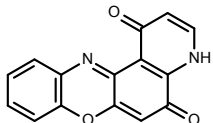
967 **Fig 8. Proposed biosynthetic pathway of ommochromes through the formation of uncyclized xanthommatin in**
968 **ommochromosomes.** See text for more details on each step. Relative sizes of arrows are indicative of reaction rates. TDO,
969 tryptophan 2,3-dioxygenase. KMO, kynurenine 3-monooxygenase. St, ABC transporter scarlet. W, ABC transporter white.
970 PHS, phenoxazinone synthase. HKT, 3-hydroxykynurenine transaminase.

A

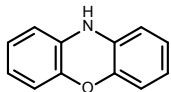
ortho-aminophenol



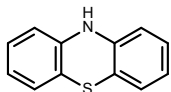
Amino-phenoxazinone



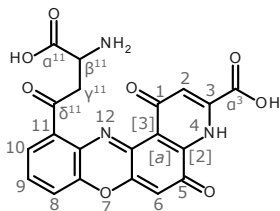
Oxo-pyrido[3,2-*a*]-phenoxazinone



Phenoxazine



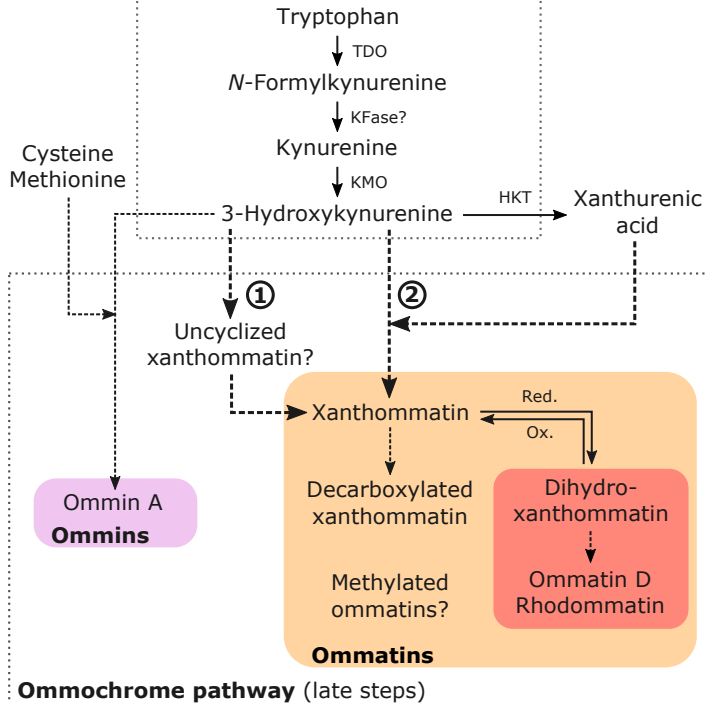
Phenothiazine



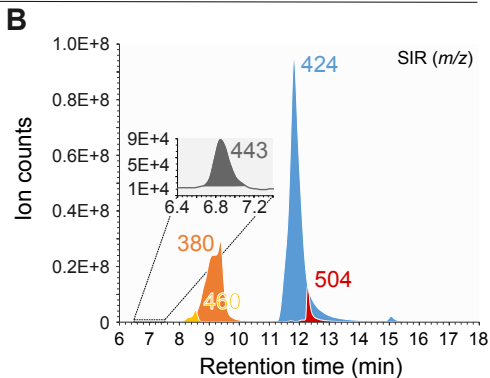
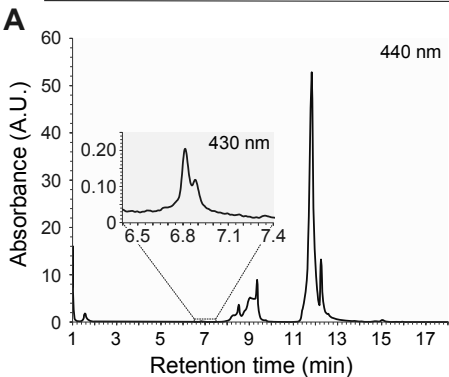
Xanthommatin

B

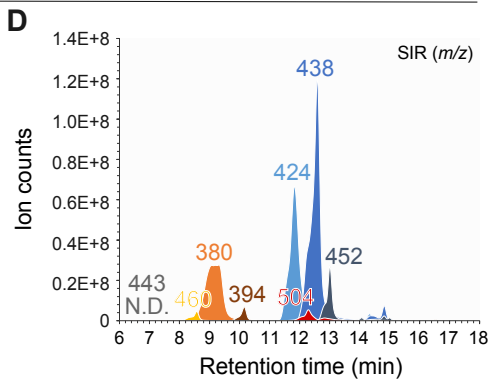
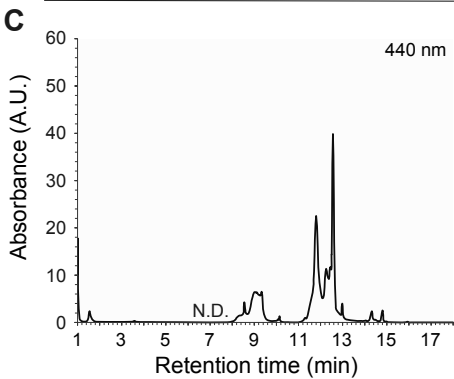
Kynurenine pathway (early steps)

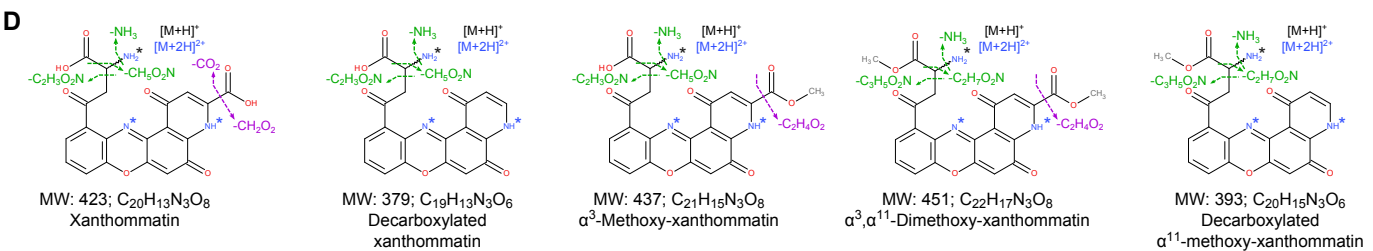
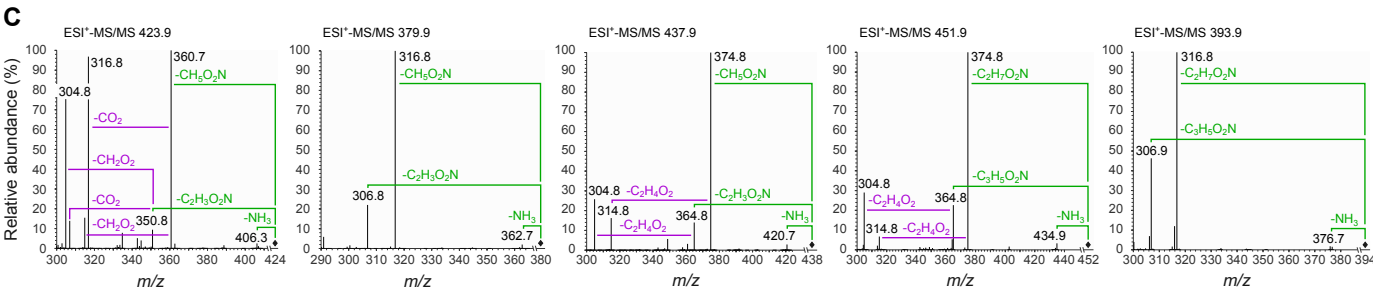
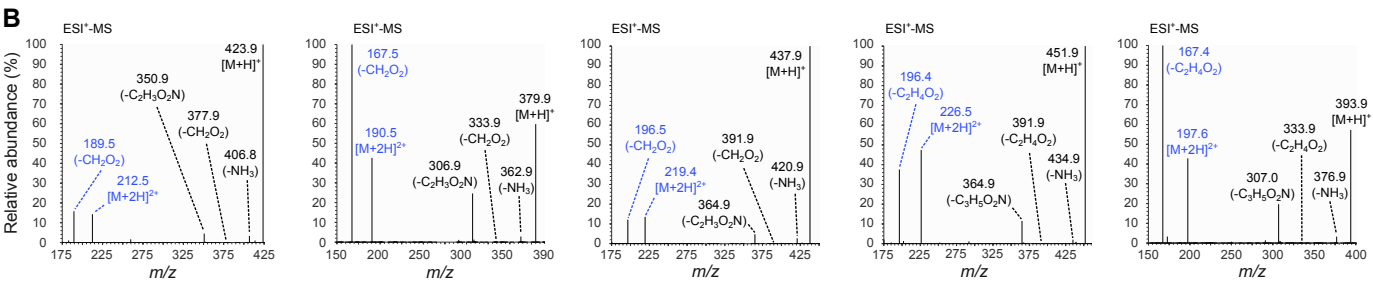
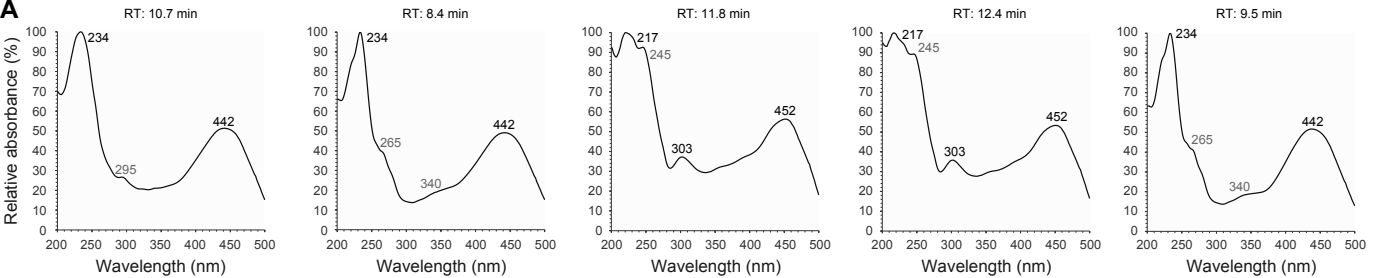


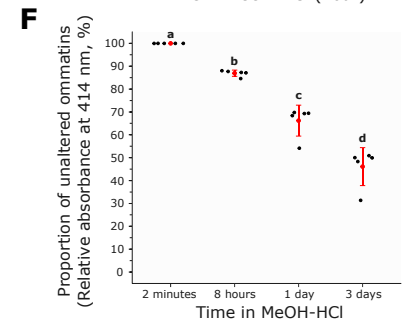
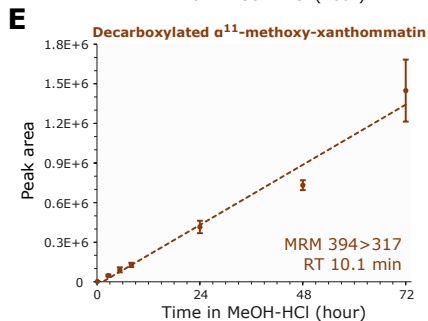
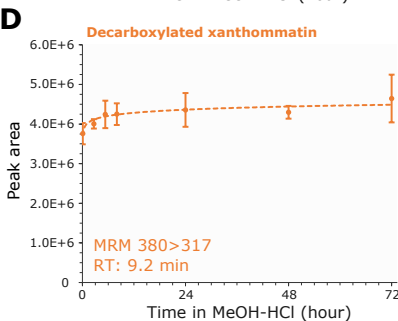
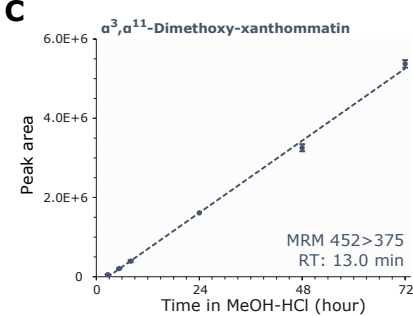
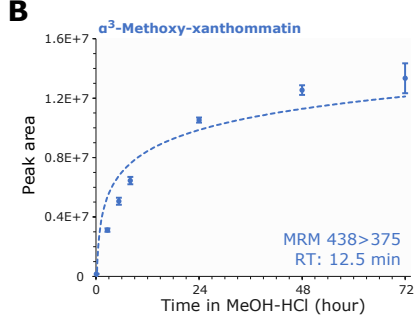
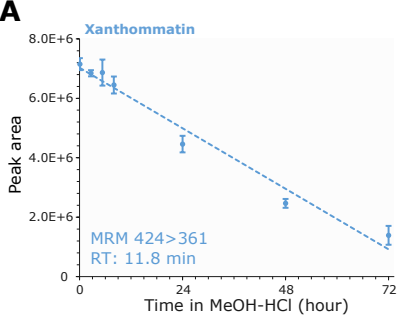
2 minutes in MeOH-HCl

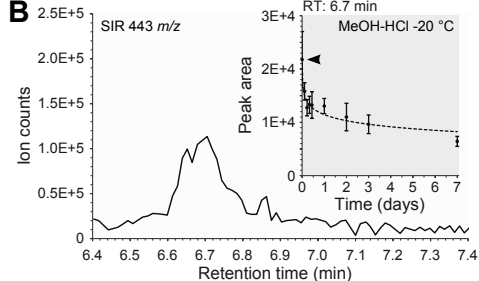
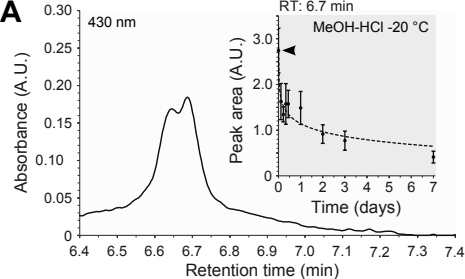


24 hours in MeOH-HCl

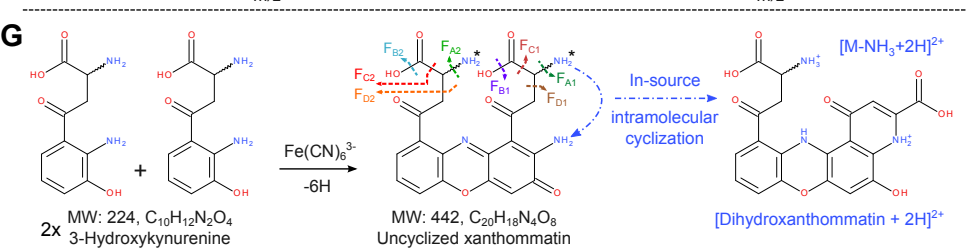
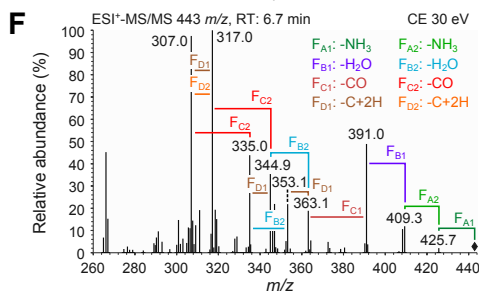
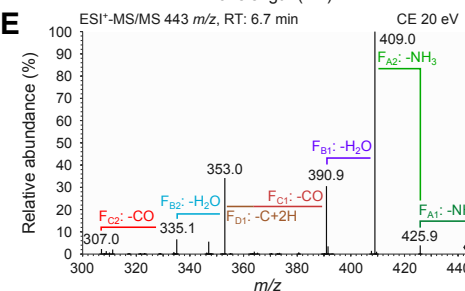
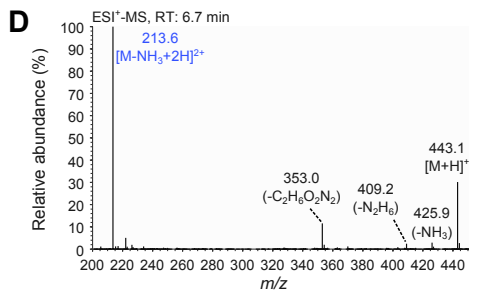
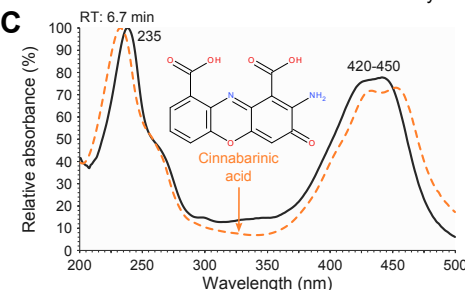








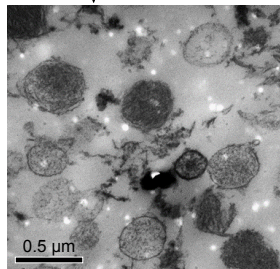
Analytical characterization



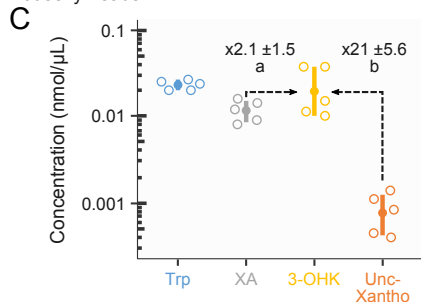
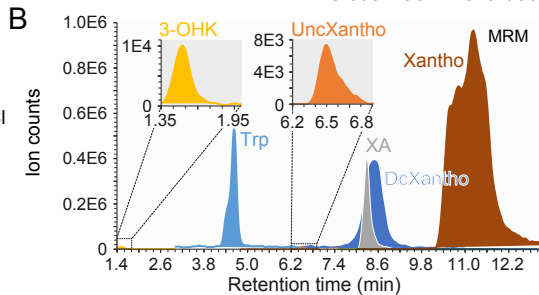


MeOH-HCl

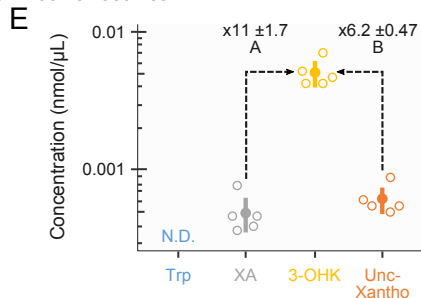
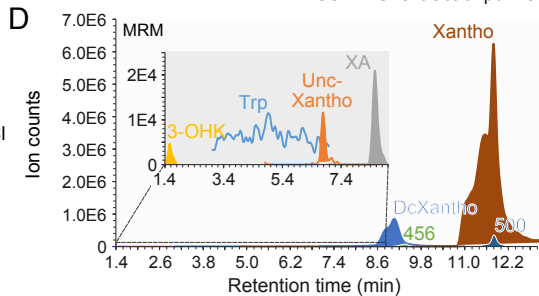
Purification of ommochromasomes

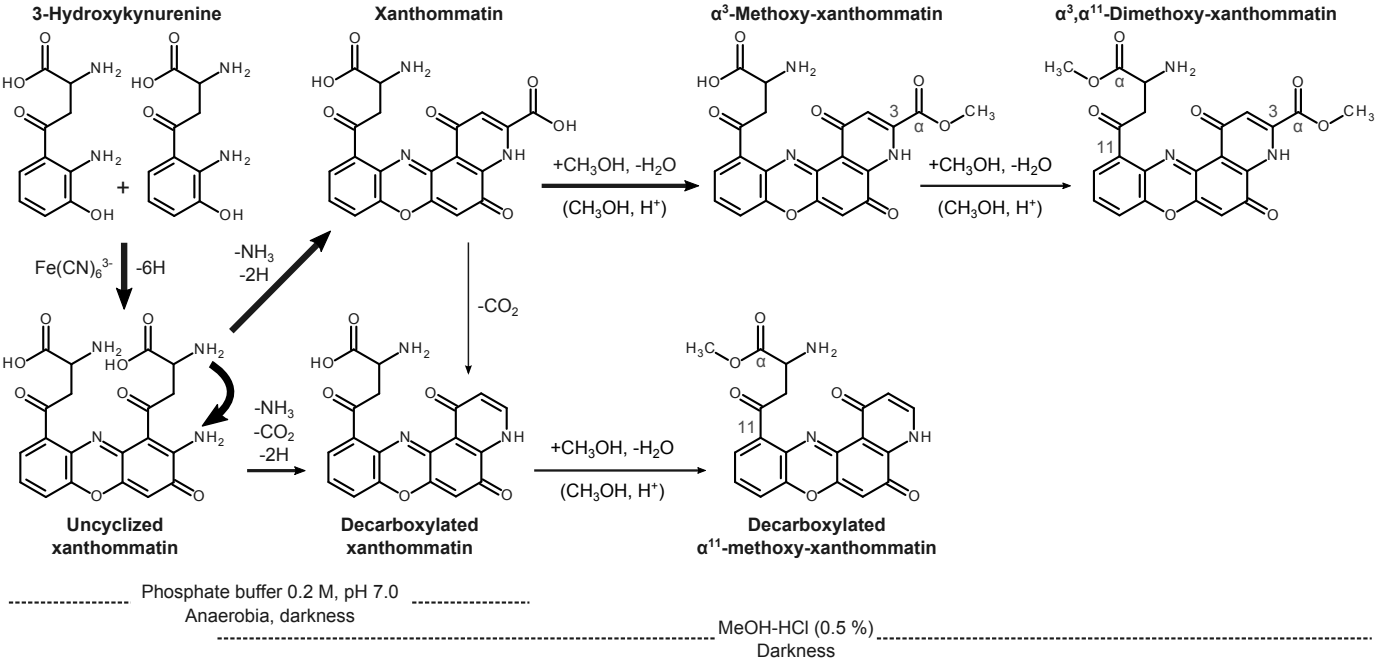


MeOH-HCl



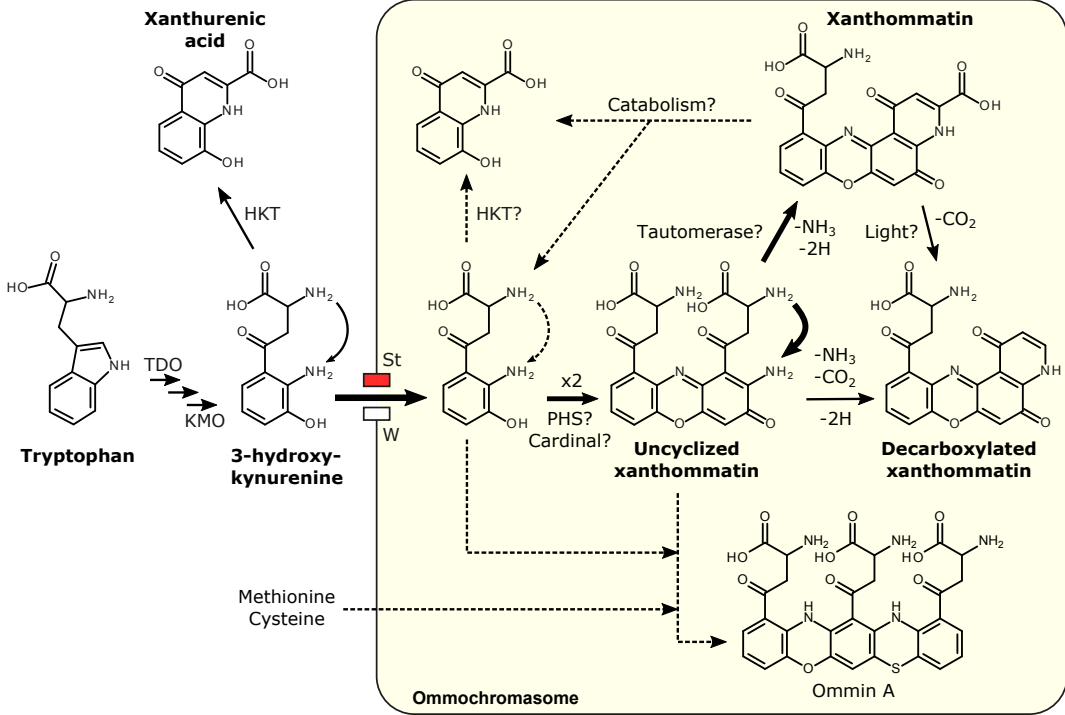
MeOH-HCl extract of purified ommochromasomes



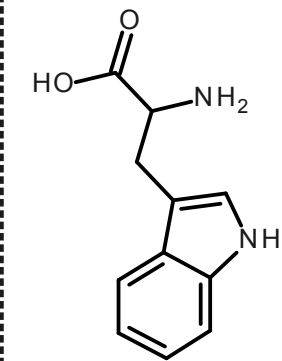


----- Kynurenine pathway -----

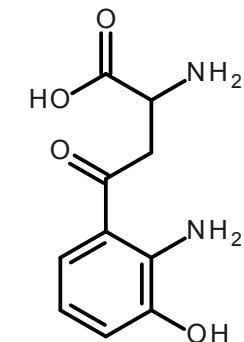
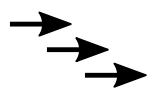
----- Ommochrome pathway -----



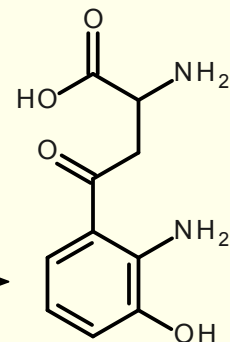
Kynurenine pathway



Tryptophan



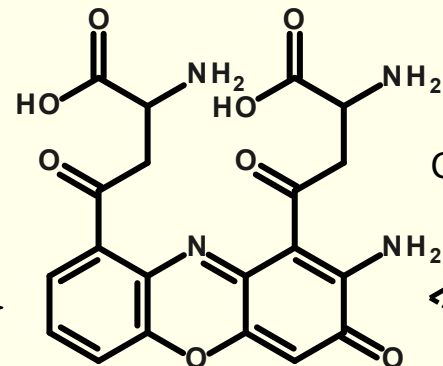
3-hydroxy-kynurenine



Dimerization

Ommochrome pathway

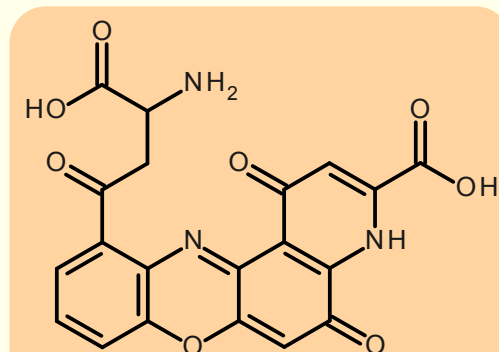
Uncyclized xanthommatin



Cyclization

New identified metabolite:

Organic synthesis + Chemical behavior
Tandem mass spectrometry + UV-Visible spectroscopy



Ommatins

Ommins



Cytosol

Ommochromasome